

# A calculation of the $B_B$ parameter in the static limit

Joseph Christensen, Terrence Draper and Craig McNeile \*

*Department of Physics and Astronomy, University of Kentucky, Lexington, KY 40506, USA*

## Abstract

We calculate the  $B_B$  parameter, relevant for  $\overline{B}^0-B^0$  mixing, from a lattice gauge theory simulation at  $\beta = 6.0$ . The bottom quarks are simulated in the static theory, the light quarks with Wilson fermions. Improved smearing functions produced by a variational technique, MOST, are used to reduce statistical errors and minimize excited-state contamination of the ground-state signal. We obtain  $B_B(4.33 \text{ GeV}) = 0.98^{+4}_{-4}$  (statistical)  $^{+3}_{-18}$  (systematic) which corresponds to  $\widehat{B}_B = 1.40^{+6}_{-6}$  (statistical)  $^{+4}_{-26}$  (systematic) for the one-loop renormalization-scheme-independent parameter. The systematic errors include the uncertainty due to alternative (less favored) treatments of the perturbatively-calculated mixing coefficients; this uncertainty is at least as large as residual differences between Wilson-static and clover-static results. Our result agrees with extrapolations of results from relativistic (Wilson) heavy quark simulations.

12.38.Gc, 14.40.Nd, 12.39.Hg, 12.38.Bx

Typeset using REVTeX

---

\*Now at Department of Physics, University of Utah, Salt Lake City, UT 84112

## I. INTRODUCTION

The experimental observation of  $\overline{B}^0-B^0$  mixing allows, in principle, the extraction of the  $|V_{td}|$  CKM matrix element [1,2]. The over-determination of the CKM matrix is a high-precision test of the standard model of particle physics and is regarded as a potential harbinger of new physics. The dominant uncertainty in the extraction of  $|V_{td}|$  from experimental measurements is due to theoretical factors from non-perturbative QCD. The key factor is  $B_B f_B^2$ , where  $f_B$  is the  $B$ -meson semi-leptonic decay constant and  $B_B$  is the “bag constant” for the  $B$ -meson, defined as the ratio of the matrix element of the operator relevant for the mixing to its value in the vacuum-saturation approximation (VSA).

There have been a large number of lattice gauge theory simulations which have calculated the  $f_B$  decay constant; however, much less work has been done on the calculation of the  $B_B$  parameter. The earliest result [3] suggested that the VSA works quite well; this result was unanticipated and is quite non-trivial, as was reiterated by Soni [2]. Later results by other groups are surprisingly scattered, with significant disagreement in some cases [4] and with some results markedly different than that suggested by VSA. Here we argue that, in fact, most raw lattice data are consistent with VSA (including ours which are quite precise due to the use of improved smearing functions) and that groups differ due to their choices of how to relate these to the full-theory continuum value. We argue that although large systematic uncertainties remain due to unknown higher-order contributions in the mixing coefficients, it is possible to formulate the calculation in a way which is stable against changes in normalization (such as tadpole improvement). Our result is in accord with VSA and is also in agreement with the large-mass extrapolation of calculations [2] which use relativistic, rather than static, heavy quarks.

Some of the first attempts at simulating the static theory calculated both the decay constant and the  $B_B$  parameter [5,6]. However, the required perturbative matching coefficients were not known; these have since been computed by Flynn *et al.* [7]. Their analysis showed that additional operators, not included in the first simulations, are required to estimate the  $B_B$  parameter.

Until recently, the simulation of the static theory was problematic because of excited-state contamination of the ground-state signal [8,9,10]. The development of variational techniques [11,12] has finally allowed a reliable extraction of the decay constant. In this paper, we use a modern variational technique [12] to obtain accurate estimates of the lattice matrix elements and combine these with the mixing coefficients to calculate the static  $B_B$  parameter. At two conferences [13,14], we have reported preliminary results for the value of  $B_B$  from this simulation.

Sec. II outlines the method of extracting the relevant matrix elements from lattice correlation functions; Sec. III summarizes our numerical results. Sec. IV contains a summary of the perturbative-matching techniques which, rather explicitly, details our preferred way of organizing the calculation; we argue that our method reduces systematic errors in the matching coefficients which are then estimated in Sec. V. In Sec. VI, a comparison is made to other groups as an illustration of the differences in the methods discussed in Sec. V. The conclusion follows as Sec. VII.

## II. NUMERICAL TECHNIQUES

The static-light  $B_B$  parameter is obtained from a combination of two- and three-point hadronic correlation functions. The required three-point function is

$$C_{3,X}(t_1, t_2) = \sum_{\vec{x}_1} \sum_{\vec{x}_2} \left\langle 0 \left| \mathcal{T} \left( \chi(t_1, \vec{x}_1) \mathcal{O}_X(0, \vec{0}) \chi(t_2, \vec{x}_2) \right) \right| 0 \right\rangle \quad (2.1)$$

which has a fermion operator inserted at the spacetime origin between two external  $B$ -meson operators,  $\chi$ . The times are restricted to the range  $t_1 > 0 > t_2$ . We use the spatially extended  $B$ -meson interpolating field

$$\chi(\vec{x}, t) = \sum_{\vec{r}} f(\vec{r}) \bar{q}(t, \vec{x} + \vec{r}) \gamma_5 b(t, \vec{x}) \quad (2.2)$$

where  $f$  is a smearing function chosen [12] to project out the ground state efficiently. The four-fermion operators,  $\mathcal{O}_X$  (with  $X \in \{L, R, N, S\}$ ), are defined<sup>1</sup> as [7]:

$$\begin{aligned} \mathcal{O}_L &= \bar{b}\gamma_\mu(1 - \gamma_5)q \bar{b}\gamma_\mu(1 - \gamma_5)q \\ \mathcal{O}_R &= \bar{b}\gamma_\mu(1 + \gamma_5)q \bar{b}\gamma_\mu(1 + \gamma_5)q \\ \mathcal{O}_N &= \left( 2\bar{b}(1 - \gamma_5)q \bar{b}(1 + \gamma_5)q + 2\bar{b}(1 + \gamma_5)q \bar{b}(1 - \gamma_5)q \right. \\ &\quad \left. + \bar{b}\gamma_\mu(1 - \gamma_5)q \bar{b}\gamma_\mu(1 + \gamma_5)q + \bar{b}\gamma_\mu(1 + \gamma_5)q \bar{b}\gamma_\mu(1 - \gamma_5)q \right) \\ \mathcal{O}_S &= \bar{b}(1 - \gamma_5)q \bar{b}(1 - \gamma_5)q \end{aligned} \quad (2.3)$$

The operators  $\mathcal{O}_R$  and  $\mathcal{O}_N$  are introduced in the lattice and contribute towards  $\mathcal{O}_L$  because of the poor chiral behavior of Wilson quarks. The operator  $\mathcal{O}_S$  is introduced in the continuum and contributes because of the matching of full QCD to the static theory.

With the smeared-sink-local-source (SL) two-point function defined as

$$C_2(t_1) = \sum_{\vec{x}_1} \left\langle 0 \left| \mathcal{T}(\chi(t_1, \vec{x}_1) \bar{b}(0, \vec{0}) \gamma_4 \gamma_5 q(0, \vec{0})) \right| 0 \right\rangle \quad (2.4)$$

the “raw” lattice-static parameters,  $B_X$ , are calculated via the ratio of three- and two-point functions:

$$B_X(t_1, t_2) = \frac{C_{3,X}(t_1, t_2)}{\frac{8}{3}C_2(t_1)C_2(t_2)} \xrightarrow{|t_i| \gg 1} B_X \quad (2.5)$$

The  $B_B$  parameter itself can then be determined from the  $B_X \equiv B_{\mathcal{O}_X}$ , extracted from fits of the Monte Carlo data to the form of Eq. (2.5), as the linear combination

$$B_B = Z_{B_L}B_L + Z_{B_R}B_R + Z_{B_N}B_N + Z_{B_S}B_S \quad (2.6)$$

---

<sup>1</sup>We choose a standard normalization for which the VSA value for  $\mathcal{O}_L$  is  $(8/3)f_B^2 m_B^2$ .

where the perturbatively-calculated mixing coefficients,  $Z_{B_X}$ , are defined in Sec. IV. Rather than this “fit-then-combine” method, our quoted results will be from the “combine-then-fit” method:

$$B_B(t_1, t_2) = \sum_{X=L,R,N,S} Z_{B_X} B_X(t_1, t_2) \xrightarrow{|t_i| \gg 1} B_B \quad (2.7)$$

For infinite statistics, the two methods should give identical results.

We exploit time-reversal symmetry by averaging the correlators over  $t$  and  $T - t$ , where  $T$  is the length of the lattice in the time direction. We fix one of the times,  $t_1$ , in Eqs. (2.5) and (2.7) and vary the other,  $t_2$ ; the result is fitted to a constant. The fits include correlations in time, but not in the chiral extrapolation (a choice forced upon us by our limited statistics). The entire fitting procedure is bootstrapped (see, for example, Ref. [15]) to provide robust estimates of the statistical errors. An estimate of the systematic error due to the choice of interval is made by calculating the variance of the results from using all “reasonable” time intervals around our favorite one.

A major problem with simulations that include static quarks is that the signal-to-noise ratio decreases very quickly with time [8,16,17]; therefore, the operator which creates the  $B$ -meson must project onto the ground state at very early times — before the signal is lost in the noise. Experience with the calculation of the  $f_B$  decay constant in the static theory has shown that reliable results can be obtained only if the  $B$ -meson operator is smeared with a very accurate “wave function,” which can be obtained from a variational calculation on the lattice. We use the same smearing function as was used in our calculation of  $f_B$  in the static approximation. This was obtained from the variational technique, called MOST [12], which we have developed for this purpose.

To demonstrate the effectiveness of the smearing function produced by MOST, we show in Fig. 1 the effective-mass plot ( $\ln C_2^{LS}(t)/C_2^{LS}(t+1)$  versus  $t+1/2$ ) for the two-point correlation function using a local (delta-function) sink at time  $t$  and an optimally-smeared source at time 0. The effective-mass plot has plateaued at small  $t$  (indicating the absence of significant excited-state contamination) before the signal-to-noise ratio has degenerated, so that a very precise mass and amplitude can be obtained by fitting over an early time range. If, instead, the same smearing function is used at the sink, with a local (delta-function) source, then it will still effectively remove excited-state contamination. Yet, as demonstrated in Fig. 2, this fact is obscured by much larger statistical fluctuations. (Since the spatial points are summed over at the sink to project out zero momentum regardless of which smearing function is used, smearing at the sink provides only marginal improvement in the signal and increases noise. In contrast, smearing at the source greatly enhances the signal and decreases the noise. For the local source the static quark is restricted to the spatial origin, and thus the statistics are poorer [9].)

We note that once an “optimal” smearing source has been obtained from the two-point function using a variational technique, it can be used directly in other calculations. The three-point function does not need to be formulated as a variational problem, although ground-state dominance should still be monitored using the mass splitting between the excited and ground states.

The static quark never evolves in space from the origin because the four-fermion operator is at the spacetime origin. The  $B$ -meson operator is constructed by smearing the light

quark relative to the heavy quark (Eq. (2.4)). Fig. 3 shows a schematic of the quark flow resulting from the Wick contraction of Eq. (2.1). The resulting two-point correlators are smeared-sink–local-source (SL) correlators, which are much more noisy than local-smeared (LS) correlators (as argued above) even though in the infinite-statistics limit they are equal. Since three-point functions are, in general, noisier than two-point functions, the “effective-mass” plots for these are even noisier than that for the SL two-point function; it would be hopeless to get a precise result for a static-light-meson matrix element without using a prohibitively large number of configurations. But fortunately, because the  $B_B$  parameter is a *ratio* of matrix elements (Eq. (2.5)), the noise is reduced due to the cancelation of correlated fluctuations between the numerator and denominator.

It has been argued that the product  $B_B f_B^2$  and perturbative corrections to it should be calculated directly since it, rather than  $B_B$ , is the phenomenologically-important quantity. But there are several compelling reasons for calculating  $f_B$  and  $B_B$  separately. Firstly, although the calculation of  $B_B$ , as for  $B_B f_B^2$ , is intrinsically more involved than is that of  $f_B$  (both analytically, in the determination of perturbative corrections, and computationally), the numerical value of  $B_B$  is more stable than is the value of either  $B_B f_B^2$  or  $f_B$ . Certainly,  $f_B$  is a very important physical quantity in its own right; it should be and is calculated separately. For this, one need only calculate a two-point function. However, the statistical fluctuations for  $f_B$  are quite large; without the use of a reliable smearing function obtained variationally, excited-state contamination can be substantial and can mislead interpretation. (This may explain the scatter in the world summary of lattice calculations of  $f_B$  [9,10].) Also, since its lattice-spacing dependence is rather large, especially when using the static approximation, its continuum extrapolation is delicate and prone to large systematic errors. Much computing effort is required to evaluate this simple quantity. However,  $B_B$  (or  $B_B f_B^2$ ) requires the calculation of a three-point, in addition to a two-point, correlation function. Since it is more involved, it is usually determined in a secondary calculation after the primary calculation of  $f_B$  and so fewer groups are likely to calculate it. Yet, as borne out by our data, since  $B_B$  can be extracted from a ratio of three- to two-point functions which are strongly correlated, a quite precise value can be obtained, with an optimal choice of smearing function, from relatively few configurations. The calculational overhead (both computational and analytical) is large compared to the computational expense. Thus a handful of groups can fix precisely the value of  $B_B$  once and for all, leaving for the wider community the task of applying improvements in algorithms and computers to the simpler  $f_B$ . In the future,  $B_B$  (in contrast to  $f_B$  and  $B_B f_B^2$ ) need not be recalculated with every generation of improvements.

Secondly, just as the numerical value of  $B_B$  is stable because of cancelations of correlated fluctuations in numerator and denominator, we argue that so too are its perturbative corrections when linearized as is demonstrated in Sections IV and V. The perturbatively-calculated coefficients for  $B_B$  are likely more reliable than those for the product  $B_B f_B^2$ . Likewise, these are less likely to need updating with the next generation of improvements in analytic methods.

Thirdly, it seems as though VSA is a surprisingly good approximation for the  $B_B$  parameter. This is an important qualitative statement, of use to model builders, which should not be obscured by poor-statistics attempts to calculate the product  $B_B f_B^2$ .

### III. NUMERICAL RESULTS

The simulations were carried out on a  $20^3 \times 30$  lattice, calculated on 32 gauge configurations, at  $\beta = 6.0$ . (This number of configurations is more than adequate for a precise estimate of the  $B_B$  parameter with small statistical error since an efficient smearing function is used. The use of an *ad hoc* smearing function would have required an order of magnitude more configurations.) The simulations were quenched; the gauge configurations were generated using the standard Wilson pure-gluon action. The gauge configurations were fixed into Coulomb gauge. (An ultra-conservative gauge-fixing convergence criterion was used such that  $\vec{\nabla} \cdot \vec{A}$  was decreased to less than  $10^{-9}$  its unfixed value.) The gauge-fixing was done only to choose smearing functions, but since these cancel in ratios of correlation functions all results are gauge-invariant (in the infinite-statistics limit). Wilson light-quark propagators, with hopping-parameter values,  $\kappa = 0.152, 0.154, 0.155$ , and  $0.156$ , were used in our analysis. The value of kappa-critical used was  $0.157$  and the value of kappa-strange was  $0.155$  [18].

Fig. 4 shows, for the operator  $\mathcal{O}_L$ , the ratio of the three- and two-point correlation functions  $B_L(t_1, t_2)$ , Eq. (2.5), which asymptotically equals  $B_L$  for large Euclidean times. (In the figure  $B_L(t_1, t_2)$  is graphed as a function of  $t_2$  with  $t_1 = -2$  held fixed.) In fact, “large times” are remarkably small ( $> \approx 2$ ) because of the effectiveness of the smearing function in efficiently eliminating excited-state contamination, a fact supported by Fig. 1.

As with any lattice calculation of correlation functions, there is freedom in the choice of fit range and a balance needs to be struck between fitting over too-early times, for which systematic errors due to excited-state contamination may be non-negligible, and over too-late times, for which statistical errors will be unnecessarily large. In Fig. 5 we display a  $t_{\min}$ -plot: the values for the fits of the raw  $B_L$  value (at  $\kappa = 0.156$ ) plotted for several choices of fit range. (All of our fits take into account the correlations in Euclidean time using the full-covariance matrix. For our central fit range, the values of the fits differ little whether or not the correlations are included.) The flatness of the plateau in Fig. 4 reflects the insensitivity of the fitted value to the choice of fit range. For this and other plots we choose as our central values  $t_1 = -2$  and  $3 \leq t_2 \leq 6$ , a moderately-aggressive choice which has good  $\chi^2/\text{dof}$  ( $0.83/3, 0.59/3, 0.41/3, 0.68/3$  for  $\kappa = 0.152, 0.154, 0.155, 0.156$ , respectively), small statistical errors, and fit-range systematic errors which are smaller than, but comparable to, the statistical errors. The fit-range systematic errors are determined from the standard deviation of all “reasonable choices.”

Figs. 6, 7, and 8 show similar plots for the raw lattice values for  $B_R$ ,  $B_N$  and  $B_S$ , respectively. Fig. 9 shows the ratio of correlation functions defined in Eq. (2.7) from which the desired  $B_B$  parameter is extracted. Again, the plot plateaus early with small statistical errors. Fig. 10 shows that, again, the value is insensitive to the choice of fit region. (For our central choice of fit range, the  $\chi^2/\text{dof}$  are  $0.74/3, 0.57/3, 0.43/3, 0.67/3$  for  $\kappa = 0.152, 0.154, 0.155, 0.156$ , respectively.) We could also calculate the final  $B_B$  parameter from the appropriate linear combination of the four fitted raw values  $B_L$ ,  $B_R$ ,  $B_N$  and  $B_S$ , as in Eq. (2.6). The  $\chi^2/\text{dof}$  are good for  $B_R$  ( $0.71, 0.67, 0.55, 0.33$ ) and  $B_N$  ( $0.60, 0.42, 0.36, 0.40$ ). The worst  $\chi^2/\text{dof}$  are for  $B_S$  ( $1.38, 1.30, 1.14, 0.85$ ). The two procedures, combine-then-fit versus fit-then-combine, could give different answers in principle (for finite statistics), but in practice we see little difference.

	$\kappa = 0.152$	$\kappa = 0.154$	$\kappa = 0.155$	$\kappa = 0.156$	$\kappa_c = 0.157$
$B_L$	$1.01^{+2}_{-2}(1)$	$1.02^{+2}_{-2}(1)$	$1.02^{+3}_{-2}(1)$	$1.03^{+3}_{-3}(2)$	$1.03^{+3}_{-3}(2)$
$B_R$	$0.96^{+1}_{-1}(1)$	$0.96^{+1}_{-2}(2)$	$0.95^{+2}_{-2}(2)$	$0.95^{+2}_{-3}(2)$	$0.95^{+2}_{-3}(2)$
$B_N$	$0.97^{+2}_{-2}(3)$	$0.96^{+2}_{-2}(4)$	$0.96^{+2}_{-2}(4)$	$0.96^{+3}_{-2}(4)$	$0.95^{+3}_{-2}(5)$
$-\frac{8}{5}B_S$	$1.00^{+2}_{-1}(2)$	$1.00^{+2}_{-2}(2)$	$1.00^{+2}_{-2}(3)$	$1.01^{+3}_{-3}(3)$	$1.01^{+3}_{-3}(3)$
$B_B(m_b^*)$	$0.95^{+2}_{-2}(1)$	$0.96^{+3}_{-2}(2)$	$0.96^{+3}_{-3}(2)$	$0.98^{+4}_{-4}(2)$	$0.98^{+4}_{-4}(3)$

TABLE I. The raw lattice  $B$  parameters for the operators  $\mathcal{O}_L$ ,  $\mathcal{O}_R$ ,  $\mathcal{O}_N$ , and  $\mathcal{O}_S$  which appear in the lattice-continuum matching, and the linear combination  $B_{\mathcal{O}_L^{\text{full}}} \equiv B_B$  as a function of  $\kappa$  and extrapolated to  $\kappa_c$ . The first errors are statistical (bootstrap) and the second are systematic due to choice of fit range. Note that  $\mathcal{O}_S$  has a VSA value different from that of  $\mathcal{O}_L$ ; with our normalization for the raw  $B$  parameters (a common denominator equal to the VSA value of  $\mathcal{O}_L$ )  $-\frac{8}{5}B_S$  would identically equal 1 if VSA were exact.

As shown in Table I, each raw lattice  $B$  parameter is close to 1.0 with small statistical errors, so our final value<sup>2</sup> for  $B_B(m_b^*)$  is also close to 1.0, the VSA value, with similarly small statistical errors.

#### IV. PERTURBATIVE MATCHING

To calculate the continuum value of the  $B_B$  parameter, our “raw” lattice results, listed in Table I, must be multiplied by a lattice-to-continuum perturbative matching coefficient. After we finished the first analysis of our data [13], we found that our value for  $B_B$  was approximately 30% higher than the result of a similar simulation by the UKQCD collaboration [21]. We suspected that this difference was due to more than just the difference in the actions. This motivated us to do a very careful study of the perturbative matching, using the results in the literature, so that we obtained the “best value” of  $B_B$  using the information available to us. (This is discussed further in Secs. V, VI, and VII.) We also studied the systematic errors in the perturbative matching to find the reason for the disagreement between UKQCD’s result and ours.

For convenience, we shall refer to the  $\Delta B = 2$  effective Hamiltonian, obtained from the standard model by integrating out the top quark and the heavy vector gauge bosons, as the “full” theory although this is also an effective field theory. The perturbative matching is broken into two stages: full QCD to the continuum-static theory and the continuum-static theory to the lattice-static theory. For the matching of full QCD to the continuum-static theory, the relevant perturbative results have been calculated to do a next-to-leading-order analysis of the  $\log(\mu/m_b)$  terms. The use of renormalization-group-improved perturbation

---

<sup>2</sup>  $B_B$  is evaluated at  $m_b^*$ , which is the scale at which the running mass is  $m(m_b^*) = m_{b_{pole}} = 4.72 \text{ GeV}$  [11,19,20].

theory reduces the renormalization-scheme dependence and the effects of the different ways of defining  $\gamma_5$  in dimensional regularization [22]. Two scales are necessary for the perturbative matching: the scale,  $\mu_b = O(m_b)$ , of the matching to the full theory (we choose  $\mu_b = m_b^*$ , where  $m_b^*$  is defined as mentioned earlier in footnote 2) and the scale,  $\mu$ , of the matching to the lattice theory (we choose  $\mu = q^*$ , which is determined from the Lepage-Mackenzie scale formulation [23] as discussed later in this section). Also, as emphasized by Ciuchini *et al.* [24], it is important to check the stability of the perturbative coefficient at next-to-leading order as the renormalization scale is changed.

We choose, as do others [21,25,26], to evaluate the full-theory operator,  $\mathcal{O}^f$ , at  $\mu_b$ :

$$\langle \mathcal{O}^f(\mu_b) \rangle = \sum_{i=L,S} C_i^{fc}(\mu_b; \mu) \langle \mathcal{O}_i^c(\mu) \rangle \quad (4.1)$$

where terms of order  $1/m$  have been dropped. We use a double-argument notation similar to Ref. [26] to emphasize that this matching of the continuum-static theory to the full theory involves two theories ( $f$  and  $c$ ) and two scales ( $\mu_b$  and  $\mu$ ).  $C_i^{fc}(\mu_b; \mu)$  includes a running of the scale in the continuum-static theory which can be written explicitly due to the form of the solution to the renormalization group equation (RGE) for the coefficients (see, for example, [27]).

$$\begin{aligned} C_i^{fc}(\mu_b; \mu) &= C_j^{fc}(\mu_b; \mu_b) \left( \mathcal{T}_g \exp \left\{ - \int_{g^c(\mu)}^{g^c(\mu_b)} d\bar{g} \frac{\hat{\gamma}^c(\bar{g})}{\beta^c(\bar{g})} \right\} \right)_{ji} \\ &\equiv C_j^{fc}(\mu_b; \mu_b) \left( \hat{U}^T \right)_{ji}^c(\mu_b, \mu) \end{aligned} \quad (4.2)$$

Since we focus on the transformation of the operators, we treat the coefficients,  $C$ , as a row vector and transpose ( $T$ ) the matrix  $U$  to be consistent with the common notation for  $U$  [28,29] which treats the coefficients as a column vector:  $(C^T)_i^{cf}(\mu; \mu_b) = \hat{U}_{ij}^c(\mu, \mu_b) (C^T)_j^{cf}(\mu_b; \mu_b)$  for which

$$\hat{U}^c(\mu, \mu_b) = \mathcal{T}_g \exp \left( \int_{g^c(\mu_b)}^{g^c(\mu)} d\bar{g} \frac{\hat{\gamma}^{cT}(\bar{g})}{\beta^c(\bar{g})} \right) \quad (4.3)$$

The superscript-label  $c$  indicates that the variables are for the continuum-static theory in which some degrees of freedom have been removed. Notice that the continuum-static scale-evolution matrix scales only the static-theory argument of the coefficient. Thus, Eq. (4.1) becomes

$$\langle \mathcal{O}^f(\mu_b) \rangle = \sum_{i,j=L,S} C_i^{fc}(\mu_b; \mu_b) \left( \hat{U}^T \right)_{ij}^c(\mu_b, \mu) \langle \mathcal{O}_j^c(\mu) \rangle \quad (4.4)$$

which is read, right-to-left, as “The static theory operator is scaled from  $\mu$  to  $\mu_b$  where it is matched to the full theory.”

An alternative, not used here, is to evaluate the full theory operator at the same scale  $\mu$  as is the static-theory operator, so that

$$\begin{aligned} \langle \mathcal{O}^f(\mu) \rangle &= \sum_{i=L,S} C_i^{fc}(\mu; \mu) \langle \mathcal{O}_i^c(\mu) \rangle \\ &= \sum_{i,j=L,S} \left( \hat{U}^T \right)^f(\mu, \mu_b) C_i^{fc}(\mu_b; \mu_b) \left( \hat{U}^T \right)_{ij}^c(\mu_b, \mu) \langle \mathcal{O}_j^c(\mu) \rangle \end{aligned} \quad (4.5)$$



(The generalization to multiple full-theory operators would include full-theory subscripts on  $\mathcal{O}^f$ ,  $(\hat{U}^T)^f$ , and  $C_i^{fc}$ .) Eq. (4.5) reads, right-to-left, “The continuum-static theory operator is scaled in the static theory from  $\mu$  to  $\mu_b$  where it is matched the full theory and then scaled back from  $\mu_b$  to  $\mu$  in the full theory.” If  $U$  is treated to lowest order, summing neither the leading nor sub-leading order logarithms, then this reduces to the approach used by Flynn *et al.* [7] who do not use the RG. The full-theory anomalous dimension appears there since this approach includes running the scale in the full theory.

Returning to Eqs. (4.1) and (4.4), matching in the continuum (with  $\mu_b = m_b^*$  and  $\mu = q^*$ ) gives

$$\langle \mathcal{O}^f(m_b^*) \rangle = C_L^{fc}(m_b^*; q^*) \langle \mathcal{O}_L^c(q^*) \rangle + C_S^{fc}(m_b^*; q^*) \langle \mathcal{O}_S^c(q^*) \rangle \quad (4.6)$$

We use the solution of the RG equation for a matrix of operators which is discussed by Ciuchini *et al.* [25] and Buchalla [26] in more detail.

$$\begin{aligned} C_L^{fc}(m_b^*; q^*) &= C_L^{fc}(m_b^*; m_b^*) \left( \frac{\alpha_s^c(m_b^*)}{\alpha_s^c(q^*)} \right)^{p_{0,L}^c} \left\{ 1 + \frac{\alpha_s^c(m_b^*) - \alpha_s^c(q^*)}{4\pi} p_{1,L}^c \right\} \\ &\quad + C_S^{fc}(m_b^*; m_b^*) \frac{\gamma_{0,S,L}^c}{\gamma_{0,L,L}^c - \gamma_{0,S,S}^c} \left( \left( \frac{\alpha_s^c(m_b^*)}{\alpha_s^c(q^*)} \right)^{p_{0,L}^c} - \left( \frac{\alpha_s^c(m_b^*)}{\alpha_s^c(q^*)} \right)^{p_{0,S}^c} \right) \end{aligned} \quad (4.7a)$$

$$C_S^{fc}(m_b^*; q^*) = C_S^{fc}(m_b^*; m_b^*) \left( \frac{\alpha_s^c(m_b^*)}{\alpha_s^c(q^*)} \right)^{p_{0,S}^c} \quad (4.7b)$$

with

$$p_{0,i} = \left( \gamma_{0,i,i} / (2b_0) \right) \quad \text{and} \quad p_{1,i} = \left[ p_{0,i} \left( \gamma_{1,i,i} / \gamma_{0,i,i} - b_1 / b_0 \right) \right] \quad (4.8)$$

In Table II we list the values of the anomalous dimensions of the various operators required in this calculation (all calculated using the naive dimensional regularization scheme). The coefficients from the first and second terms of the  $\beta$ -function are defined as

$$\beta_0 \equiv \frac{b_0}{4\pi} = \frac{11 - \frac{2}{3}n_f}{4\pi}, \quad \beta_1 \equiv \frac{b_1}{16\pi^2} = \frac{102 - \frac{38}{3}n_f}{16\pi^2} \quad (4.9)$$

To obtain the leading-log expressions from the explicit solutions of the renormalization group equations that we quote, all quantities with a subscript 1 are omitted. In Eq. (4.7b) the higher-order terms of  $U^c$  have been dropped when multiplied by  $C_S^{fc}$  because  $C_S^{fc}$  is of order  $\alpha_s$ . We found that the inclusion of the  $C_S^{fc}(U^T)_{S,L}^c$  term in our analysis was less than 0.05% of the  $C_L^{fc}(U^T)_{L,L}^c$  term; this is smaller than the few percent effect which was quoted in Refs. [25,26]. Our ratio of the coupling at  $\mu$  to that at  $\mu_b$  was close to 1 because the automatic scale-setting procedure selected a scale  $q^*$  which was close to  $m_b^*$ . As the difference between the scales  $\mu$  and  $\mu_b$  gets bigger,  $(U^T)_{S,L}^c$ , which includes the leading off-diagonal terms in the anomalous dimension matrix, gets larger.

We will now discuss the matching of the continuum-static theory to the lattice-static theory. The relevant perturbative calculations have been done by Flynn *et al.* [7]. We want to calculate the full theory at  $m_b^*$ :

Ref.	their notation	our notation	value
Ciuchini <i>et al.</i> [25], Buchalla [26] Giménez [30]	$\gamma_{11}^{(0)}$ $4\gamma_+^{(1)} \Big _{\overline{MS}}$	$\gamma_{0,L}^c$	$-8$
Ciuchini <i>et al.</i> [25], Buchalla [26] Giménez [30]	$\gamma_{11}^{(1)}$ $16\gamma_+^{(2)} \Big _{\overline{MS}}$	$\gamma_{1,L}^c$	$-\frac{4}{9} \left( 202 + 26\frac{\pi^2}{6} - 16n_f \right)$
Ciuchini <i>et al.</i> [25], Buchalla [26]	$\gamma_{21}^{(0)}$	$\gamma_{0,S}^c$	$\frac{4}{3}$
Ciuchini <i>et al.</i> [25], Buchalla [26]	$\gamma_{22}^{(0)}$	$\gamma_{0,S}^c$	$-\frac{8}{3}$
Ciuchini <i>et al.</i> [25], Buchalla [26]	$d_1$	$p_{0,L}^c$	$\frac{\hat{\gamma}_{0,L,L}^c}{2b_0}$
Ciuchini <i>et al.</i> [25], Buchalla [26]	$d_2$	$p_{0,S}^c$	$\frac{\hat{\gamma}_{0,S,S}^c}{2b_0}$
Ciuchini <i>et al.</i> [25], Buchalla [26]	$-J$	$p_{1,L}^c$	$p_{0,L}^c \left( \frac{\gamma_{1,L,L}^c}{\gamma_{0,L,L}^c} - \frac{b_1}{b_0} \right)$
Duncan <i>et al.</i> [11,31,32,33,34]	$\gamma_0$ $\gamma_1$	$\gamma_{0,A}^c$ $\gamma_{1,A}^c$	$-4$ $\frac{-254}{9} - \frac{56\pi^2}{27} + \frac{20n_f}{9}$
Buras <i>et al.</i> [35]	$\gamma^0$	$\gamma_{0,L}^f$	$4$
Buras <i>et al.</i> [35]	$\gamma^1$	$\gamma_{1,L}^f$ $p_{0,A}^f$ $p_{1,A}^f$	$\left( -7 + \frac{4}{9}n_f \right)$ $0$ $0$

TABLE II. Anomalous dimensions as defined by various groups and used here. The  $p$ 's are defined in Eq. (4.8). All the results have been calculated using the naive dimensional regularization scheme.

$$\begin{aligned} \langle \mathcal{O}^f(m_b^*) \rangle &= C_L^{fc}(m_b^*; q^*) \left( Z_L^{cl}(q^*; a) \langle \mathcal{O}_L^l(a) \rangle + Z_R^{cl}(q^*; a) \langle \mathcal{O}_R^l(a) \rangle + Z_N^{cl}(q^*; a) \langle \mathcal{O}_N^l(a) \rangle \right) + \\ &+ C_S^{fc}(m_b^*; q^*) Z_S^{cl}(q^*; a) \langle \mathcal{O}_S^l(a) \rangle \end{aligned} \quad (4.10)$$

where  $Z^{cl}(q^*; a)$  relates the bare lattice-static theory matrix element to the renormalized continuum-static theory matrix element. After linearizing the product  $C^{fc}(m_b^*; q^*) Z^{cl}(q^*; a)$  and allowing a separate coupling for continuum-static ( $\alpha_s^c$ ) and for lattice-static ( $\alpha_s^l$ ) we find:

$$\begin{aligned} \langle \mathcal{O}^f(m_b^*) \rangle &= \left[ \left( \frac{\alpha_s^c(m_b^*)}{\alpha_s^c(q^*)} \right)^{p_{0,L}^c} \left( 1 + \frac{\alpha_s^c(m_b^*) - \alpha_s^c(q^*)}{4\pi} p_{1,L}^c + \frac{\alpha_s^c(m_b^*)}{4\pi} (-14) \right. \right. \\ &\quad \left. \left. + \frac{\alpha_s^l(q^*)}{4\pi} (4 \ln(q^{*2} a^2) - 21.7) \right) \right. \\ &\quad \left. - \frac{1}{4} \left( \left( \frac{\alpha_s^c(m_b^*)}{\alpha_s^c(q^*)} \right)^{p_{0,L}^c} - \left( \frac{\alpha_s^c(m_b^*)}{\alpha_s^c(q^*)} \right)^{p_{0,S}^c} \right) \frac{\alpha_s^c(m_b^*)}{4\pi} (-8) \right] \langle \mathcal{O}_L^l(a) \rangle \\ &+ \left( \frac{\alpha_s^c(m_b^*)}{\alpha_s^c(q^*)} \right)^{p_{0,L}^c} \left\{ \frac{\alpha_s^l(q^*)}{4\pi} (-1.61) \langle \mathcal{O}_R^l(a) \rangle + \frac{\alpha_s^l(q^*)}{4\pi} (-14.4) \langle \mathcal{O}_N^l(a) \rangle \right\} \\ &+ \left( \frac{\alpha_s^c(m_b^*)}{\alpha_s^c(q^*)} \right)^{p_{0,S}^c} \frac{\alpha_s^c(m_b^*)}{4\pi} (-8) \langle \mathcal{O}_S^l(a) \rangle \end{aligned} \quad (4.11)$$

where we have updated the results of Flynn *et al.* [7] by including  $(U^T)_{S,L}^c$  [25,26], by choosing the convention that the static-light two-point function be fit to the  $Ae^{-mt}$  model [21,36], and by including tadpole improvement [37].

Throughout this paper we assume the convention that the  $f_B$  decay constant is extracted from the heavy-light correlators using the model  $Ae^{-mt}$ . Using this model changes the heavy-quark wave-function renormalization integral, denoted  $e$ , to a reduced value  $e^{(R)}$  (see Eichten and Hill [36]). As mentioned by the UKQCD collaboration [21], this changes the  $D_L = -65.5$  of Flynn *et al.* (the additive constant in the matching of the continuum-static  $\mathcal{O}_L^c$  operator to the lattice operator) to  $D_L^{(R)} = -38.9$ . However,  $e^{(R)}$  also appears in  $Z_A^{cl}$ ; thus, the final values for the coefficients of the  $B$  parameters are independent of this choice if the ratio is linearized in  $\alpha^c$  and  $\alpha^l$ . In addition, any tadpole-improvement effects alter the three-point function by twice as much as each two-point function; linearizing the ratio cancels these effects exactly. However, when considering the three-point function and two-point function separately, one ought to include the effects of tadpole improvement. This changes the  $D_L^{(R)} = -38.9$  to  $D_L^{(R,tad)} = -21.7$ , as in Eq. (4.11). The large perturbative factors of the wave-function renormalization largely cancel in the expression for the  $B_B$  parameters.

To calculate the coefficients of  $B_B$ , the renormalization coefficient of the axial current in the static approximation is required [31,32,33,34,36,38]; we linearized the results quoted in Duncan *et al.* [11]:

$$\begin{aligned} Z_A &\equiv C_A^{fc}(m_b^*; q^*) Z_A^{cl}(q^*; a) \\ &= \left( \frac{\alpha_s^c(m_b^*)}{\alpha_s^c(q^*)} \right)^{p_{0,A}^c} \left( 1 + \frac{\alpha_s^c(m_b^*) - \alpha_s^c(q^*)}{4\pi} p_{1,A}^c + \frac{\alpha_s^c(m_b^*)}{4\pi} \left( -\frac{8}{3} \right) + \frac{\alpha_s^l(q^*)}{4\pi} (2 \ln(q^{*2} a^2) - 18.59) \right) \end{aligned} \quad (4.12)$$

where the  $-18.59$  is from using the  $e^{(R)}$  mentioned above as well as including tadpole improvement. If tadpole improvement had not been used, then this value would be  $-27.16$ . If  $e$  had been used instead of  $e^{(R)}$ , then this value would be  $-40.44$ . As long as one is consistent between Eqs. (4.11) and (4.12), these effects cancel out of the linearized result for  $B_B$ .

The perturbative coefficients for the  $B_B$  parameter can be obtained by dividing the four-fermion results by the square of  $Z_A$  and expanding the expressions linearly in  $\alpha_s$ .

$$\begin{aligned}
B_B(m_b^*) = & \left[ \left( \frac{\alpha_s^c(m_b^*)}{\alpha_s^c(q^*)} \right)^{p_{0,L}^c - 2p_{0,A}^c} \left( 1 + \frac{\alpha_s^c(m_b^*) - \alpha_s^c(q^*)}{4\pi} (p_{1,L}^c - 2p_{1,A}^c) + \frac{\alpha_s^c(m_b^*)}{4\pi} \left( -\frac{26}{3} \right) \right. \right. \\
& \left. \left. + \frac{\alpha_s^l(q^*)}{4\pi} (15.41) \right) \right. \\
& - \frac{1}{4} \left( \left( \frac{\alpha_s^c(m_b^*)}{\alpha_s^c(q^*)} \right)^{p_{0,L}^c - 2p_{0,A}^c} - \left( \frac{\alpha_s^c(m_b^*)}{\alpha_s^c(q^*)} \right)^{p_{0,S}^c - 2p_{0,A}^c} \right) \frac{\alpha_s^c(m_b^*)}{4\pi} (-8) \left. \right] B_L \\
& + \left( \frac{\alpha_s^c(m_b^*)}{\alpha_s^c(q^*)} \right)^{p_{0,L}^c - 2p_{0,A}^c} \left[ \frac{\alpha_s^l(q^*)}{4\pi} (-1.61) B_R + \frac{\alpha_s^l(q^*)}{4\pi} (-14.4) B_N \right] \\
& + \left( \frac{\alpha_s^c(m_b^*)}{\alpha_s^c(q^*)} \right)^{p_{0,S}^c - 2p_{0,A}^c} \frac{\alpha_s^c(m_b^*)}{4\pi} (-8) B_S
\end{aligned} \tag{4.13a}$$

$$B_B(m_b^*) \equiv Z_{B_L} B_L + Z_{B_R} B_R + Z_{B_N} B_N + Z_{B_S} B_S \tag{4.13b}$$

where  $Z_{B_X} = \text{Lin}(Z_X/Z_A^2) = \text{Lin}\left((C_X^{fc} Z_X^{cl})/(C_A^{fc} Z_A^{cl})^2\right)$ ,  $X$  is one of  $\{L, R, N, S\}$ , and “Lin” signifies that the ratio is linearized as explained later in Sec. V. The wave-function normalization factors of the quarks cancel between the numerator and denominator; no “tadpole” factors are required for this calculation if the coefficients are linearized. We also note from the values in Table II that  $p_{0,L}^c - 2p_{0,A}^c$  is identically zero. However,  $p_{0,S}^c - 2p_{0,A}^c$  and  $p_{1,L}^c - 2p_{1,A}^c$  are not. If Eq. (4.13b) were expanded into explicit  $\ln(\mu/m_b)$  terms, then to first order the perturbative matching coefficients would not contain any logs.

To calculate numerical values of the coefficients, we choose values for the scales  $\mu_b$  and  $\mu$ , and for the couplings  $\alpha_s^c$  and  $\alpha_s^l$ . For  $\alpha_s^l$ , we use  $\alpha_V$ , the coupling introduced by Lepage and Mackenzie [23]. We use the plaquette value  $-\ln W_{11} = 0.5214$  at  $\beta = 6.0$ . In the quenched approximation ( $n_f = 0$ ),

$$-\ln(W_{11}) = \frac{4\pi}{3} \alpha_V \left( \frac{3.41}{a} \right) \left( 1 - \alpha_V \left( \frac{3.41}{a} \right) (1.19) \right) \tag{4.14}$$

which uses a lattice coupling which evolves with the form

$$\alpha_s(\mu) = \left[ \beta_0 \ln \left( \frac{\mu^2}{\Lambda^2} \right) + \frac{\beta_1}{\beta_0} \ln \left( \ln \left( \frac{\mu^2}{\Lambda^2} \right) \right) \right]^{-1} \tag{4.15}$$

where the  $\beta$  are defined in Eq. (4.9). Eq. (4.14) defines  $\alpha_V$  and gives  $\Lambda_V a = 0.169$ .

Because the continuum-to-lattice matching is known only to one loop, these perturbative expressions are sensitive in principle to the value of the scale used in the matching. This dependence can only be reduced by calculating higher-order loops. However, Lepage and

Mackenzie [23] have described a plausible procedure for determining the scale and they have successfully tested this method for a number of quantities.

The Lepage-Mackenzie scale  $q^*$  is obtained from

$$\langle \ln(qa)^2 \rangle = \frac{\int d^4q f(q) \ln(q^2)}{\int d^4q f(q)} \quad (4.16)$$

$$q^*a = \exp\left(\frac{1}{2} \langle \ln(qa)^2 \rangle\right) \quad (4.17)$$

where  $f(q)$  is the finite integrand of the lattice graphs; note that  $f(q)$  is defined by assuming that all the perturbative expressions are expanded linearly in the coupling. We used the integrands of Flynn *et al.* [7]. (These have been confirmed by Borrelli and Pittori [39].) In Table III, we show the value of the scale for several operators. Our value for the scale for the static-light axial current,  $q^*a = 2.18$ , agrees with the calculation by Hernández and Hill [37].

The Lepage-Mackenzie scales for the individual operators in Table III are all around 2.0; however, the combined operator for  $B_{\mathcal{O}_L^{\text{full}}}$  has a lower scale of 1.22. (The scale quoted for  $B_{\mathcal{O}_L^{\text{full}}}$  in the original preprint and conference proceeding [14] was incorrect.) Morningstar [40] also found very low scales for the perturbative renormalization of the quark mass in NRQCD (also see the comments by Sloan [41]); though this could be related to renormalon effects [42]. Using the scale of 1.22 gave large perturbative corrections. The Lepage-Mackenzie scale-setting procedure could be confused by taking the ratio of matrix elements of two operators that are approximately the same (obviously it would be inappropriate for the case of two equal operators because  $f$  would be identically zero). We chose to use the scale of  $2.18/a$  as this is a typical scale for both  $A_\mu$  and  $\mathcal{O}_L^{\text{full}}$ .

We used  $\Lambda_{\text{QCD}}^{(5)} = 0.175 \text{ GeV}$  from Duncan *et al.* [11]. They chose values for  $a^{-1}$  obtained from the charmonium system due to the low systematic errors. Although they do not quote a value for  $a^{-1}$  at  $\beta=6.0$ , they did extrapolate  $\Lambda_V$  from  $a^{-1}$  at  $\beta=5.7, 5.9$ , and  $6.1$  in order to find  $a^{-1}$  at  $\beta=6.3$ . We used this idea to interpolate to  $a^{-1}=2.1 \text{ GeV}$  for  $\beta=6.0$ . We also used their method for calculating  $m_b^*$ ; however, our number differs slightly because of the difference between the form of Eq. (4.15) and

$$\alpha_s(\mu) = \frac{1}{\beta_0 \ln\left(\frac{\mu^2}{\Lambda^2}\right)} \left[ 1 - \frac{\beta_1}{\beta_0^2} \frac{\ln\left(\ln\left(\frac{\mu^2}{\Lambda^2}\right)\right)}{\ln\left(\frac{\mu^2}{\Lambda^2}\right)} \right] \quad (4.18)$$

With the full-to-continuum scale set as  $\mu_b = m_b^* = 4.33 \text{ GeV}$  and the continuum-to-lattice scale set by  $\mu a = q^*a = 2.18$ , we find  $\alpha_s^c(m_b^*) = 0.21$  and  $\alpha_s^l(q^*) = 0.18$ .

Using a Monte Carlo technique, we estimated the error on the static  $B_B$  parameter due to varying the values of the parameters used in the perturbation theory. A sample of one thousand was generated using uniform deviates for the renormalization scale, lattice spacing, the continuum  $\Lambda_{\text{QCD}}$ , and the bottom quark mass. The central value for each “input”-parameter distribution was set equal to our best value, based on those used in references [11,37]. Rather than assume that the input parameters are known to three significant figures, we took up to 20% of this value to be the standard deviation for each input parameter. The final results were sorted numerically and the 68% error range was taken as the “output” error. This procedure should produce more accurate estimates of errors than naive error analysis. Table IV shows the resulting error in the coefficients. Table V shows the corresponding error

	$A_\mu$	$\mathcal{O}_L$	$\mathcal{O}_L^{\text{full}}$	$B_{\mathcal{O}_L}$	$B_{\mathcal{O}_L^{\text{full}}} = B_B$
$q^*a$	2.18	2.01	2.15	2.45	1.22

TABLE III. Renormalization scales determined by the Lepage-Mackenzie prescription for the axial-vector current  $A_\mu$ , for the raw lattice operator  $\mathcal{O}_L$ , and for  $\mathcal{O}_L^{\text{full}}$ , are similar. Using this prescription for a ratio of matrix elements (as for  $B_B$ ) is unstable, as described in the text; therefore, we choose 2.18 as the scale appropriate for  $B_B$ .

in  $B_B$ . The  $B_B$  parameter is very insensitive to rather large changes in these parameters. Variations of 20% in these parameters change the  $B_B$  parameter by less than the statistical bootstrap errors. It is particularly important that the results are not sensitive to the lattice spacing because there are a wide range of possible lattice spacings that could have been used:  $a^{-1} = 1.94 \text{ GeV}$  from the string tension [43],  $a^{-1} = 2.3 \text{ GeV}$  from the  $\rho$  mass [18], and  $a^{-1} = 2.4 \text{ GeV}$  from Upsilon spectroscopy [44].

To compare the results of  $B_B$  parameters, in the next section we list our results in terms of the one-loop and the two-loop renormalization-group-invariant parameter [35]. We also scale  $B_B$  down to  $2.0 \text{ GeV}$  for the comparison to some other groups (Sec. VI) which is discussed later.

To compare at one-loop, we scaled  $B_B$  and calculated  $\hat{B}_B$  using

$$B_B(\mu_1) = \left( \frac{\alpha_s(\mu_1)}{\alpha_s(\mu_2)} \right)^{p_{0,L}^f - 2p_{0,A}^f} B_B(\mu_2) \quad (4.19)$$

$$\hat{B}_B = \alpha_s(\mu_2)^{-(p_{0,L}^f - 2p_{0,A}^f)} B_B(\mu_2) \quad (4.20)$$

where  $p$  is defined in Eq. (4.8) with the relevant anomalous dimensions listed in Table II. Since this is a one-loop calculation, we used

$$\alpha_s^{-1}(\mu) = \beta_0 \ln \left( \left( \frac{\mu}{\Lambda} \right)^2 \right) \quad (4.21)$$

Although a one-loop calculation is traditional, one can also calculate a two-loop renormalization-group-invariant  $\hat{B}_B$  parameter since the required perturbative calculations have been done.

$$B_B(\mu_1) = \left( \frac{\alpha_s(\mu_1)}{\alpha_s(\mu_2)} \right)^{p_{0,L}^f - 2p_{0,A}^f} \left( 1 + \frac{\alpha_s(\mu_1) - \alpha_s(\mu_2)}{4\pi} (p_{1,L}^f - 2p_{1,A}^f) \right) B_B(\mu_2) \quad (4.22)$$

$$\hat{B}_B = \alpha_s(\mu_2)^{-(p_{0,L}^f - 2p_{0,A}^f)} \left( 1 - \frac{\alpha_s(\mu_2)}{4\pi} (p_{1,L}^f - 2p_{1,A}^f) \right) B_B(\mu_2) \quad (4.23)$$

Again  $p$  is defined in Eq. (4.8) and the relevant anomalous dimensions are listed in Table II. Eq. (4.15) was used to scale  $B_B$  and calculate  $\hat{B}_B$  to second order.

In making a comparison to other groups, one can use either  $B_B$  evaluated at some scale or  $\hat{B}_B$ . There are disadvantages to both. For the former, either a common scale needs to be

	$q^*a$ 2.18	$a^{-1}$ 2.1 GeV	$m_b^*$ 4.33 GeV	$\Lambda_{\text{QCD}}^{(5)}$ 0.175 GeV	All
$Z_{B_L} = 1.070$					
10%	+0.002	+0.003	+0.003	+0.0008	+0.004
	-0.002	-0.004	-0.003	-0.0005	-0.005
20%	+0.005	+0.006	+0.006	+0.0019	+0.008
	-0.003	-0.009	-0.005	-0.0009	-0.009
$Z_{B_R} = -0.0225$					
10%	+0.0005	-	-	-	+0.0005
	-0.0006	-	-	-	-0.0006
20%	+0.0009	-	-	-	+0.0009
	-0.0015	-	-	-	-0.0015
$Z_{B_N} = -0.202$					
10%	+0.005	-	-	-	+0.005
	-0.006	-	-	-	-0.006
20%	+0.008	-	-	-	+0.008
	-0.012	-	-	-	-0.012
$Z_{B_S} = -0.137$					
10%	-	-	+0.003	+0.002	+0.003
	-	-	-0.003	-0.003	-0.004
20%	-	-	+0.006	+0.005	+0.006
	-	-	-0.005	-0.007	-0.008

TABLE IV. The absolute changes from our preferred values of the coefficients  $Z_{B_L}$ ,  $Z_{B_R}$ ,  $Z_{B_N}$ , and  $Z_{B_S}$  as the parameters  $q^*a$ ,  $a^{-1}$ ,  $m_b^*$ , and  $\Lambda_{\text{QCD}}^{(5)}$ , are varied by 10% and 20% first individually, and then jointly (“All”), from our preferred values. We do not imply and need not assume that the input parameters are known to three significant figures (indeed the coefficients are quite insensitive to 20% variations in the values of the parameters); rather, we chose central values based on references [11,37].

	$\kappa = 0.152$	$\kappa = 0.154$	$\kappa = 0.155$	$\kappa = 0.156$	$\kappa_c = 0.157$
10%	+0.007	+0.007	+0.007	+0.007	+0.007
	-0.009	-0.009	-0.009	-0.009	-0.009
20%	+0.013	+0.013	+0.013	+0.013	+0.013
	-0.017	-0.017	-0.017	-0.017	-0.017

TABLE V. The absolute changes in  $B_B$ , from Eq. (2.6), due to changes in the coefficients  $Z_{B_L}$ ,  $Z_{B_R}$ ,  $Z_{B_N}$ , and  $Z_{B_S}$  as the parameters  $q^*a$ ,  $a^{-1}$ ,  $m_b^*$ , and  $\Lambda_{\text{QCD}}^{(5)}$  are varied jointly by 10% and 20% from our preferred values.

agreed upon or  $B_B$  must be scaled. For the latter, the dependence of  $\hat{B}_B$  on the choice of  $n_f$  and  $\Lambda$  is not negligible;  $\hat{B}_B$  can vary by as much as 4% to 5% (see Sec. V). This dependence is also relevant to using one-loop versus two-loop because the difference in the value of  $\Lambda^{(n_f)}$  between Eqs. (4.21) and (4.15) can vary by as much as 10%. The advantage to comparing  $B_B$  at some scale is that the dependence on  $n_f$  and  $\Lambda$  is less significant ( $\approx 1\%$ , see Table V). Also, given a value for  $B_B(m_b^*)$ , one can quote a value for  $\hat{B}_B$  using either 4 or 5 flavors since  $m_b^*$  is the boundary between  $n_f = 4$  and 5 flavors. These give different constant values of  $\hat{B}_B$  for the different flavor regimes. One should be explicit about which is quoted.

Even though the numerical results are for the quenched theory, we use  $n_f=5$  for  $\mu \geq m_b^*$  and  $n_f=4$  for  $\mu \leq m_b^*$ . There is some evidence from studies of the QCD coupling that the effects of omitting dynamical fermions can be modeled by using the correct number of flavors in the  $\beta$  function (see Sloan [41] for a review).

## V. SYSTEMATIC ERRORS IN THE MATCHING

The discussion until now has not revealed any large systematic errors in the perturbative matching that could explain the difference between our result and UKQCD's. In this section we investigate the systematic error caused by combining the perturbative coefficients for the two-point and three-point functions in different ways to form the matching coefficient for the  $B_B$  operator. The UKQCD collaboration found a 20% effect when they changed the way they organized their perturbative coefficients [21].

We consider three different ways of calculating the coefficients  $Z_{BX}$  to consider these effects. For convenience, we define the following, where  $X$  is one of  $\{L, R, N, S, A\}$ :

$$\begin{aligned} Z_X &\equiv \text{product of } (C_X^{fc} Z_X^{cl}) \\ &= \left( \frac{\alpha_s^c(m_b^*)}{\alpha_s^c(q^*)} \right)^{p_{0,X}^c} \left( 1 + \frac{\alpha_s^c(m_b^*) - \alpha_s^c(q^*)}{4\pi} p_{1,X}^c + \frac{\alpha_s^c(m_b^*)}{4\pi} (D_X^c) \right) \\ &\quad \times \left( 1 + \frac{\alpha_s^l(q^*)}{4\pi} (d_X^l \ln(q^* a)^2 + D_X^l) \right) \end{aligned} \quad (5.1)$$

$$\begin{aligned} \text{Lin}(Z_X) &\equiv \text{linearization of } (C_X^{fc} Z_X^{cl}) \\ &= \left( \frac{\alpha_s^c(m_b^*)}{\alpha_s^c(q^*)} \right)^{p_{0,X}^c} \left( 1 + \frac{\alpha_s^c(m_b^*) - \alpha_s^c(q^*)}{4\pi} p_{1,X}^c + \frac{\alpha_s^c(m_b^*)}{4\pi} (D_X^c) \right. \\ &\quad \left. + \frac{\alpha_s^l(q^*)}{4\pi} (d_X^l \ln(q^* a)^2 + D_X^l) \right) \end{aligned} \quad (5.2)$$

We wish to compare three forms of linearization: “fully linearized”  $\text{Lin}(Z_L/Z_A^2)$ , “not linearized”  $Z_L/Z_A^2$  and “partially linearized”  $\text{Lin}(Z_L)/\text{Lin}(Z_A)^2$ . The UKQCD collaboration compared their  $\text{Lin}(Z_L)/\text{Lin}(Z_A)^2$  to  $Z_L/\text{Lin}(Z_A)^2$  when they found their 20% effect in  $B_B$ . Since  $C_A^{fc}$  is very close to 1,  $\text{Lin}(Z_A)$  is approximately equal to  $Z_A$ . Thus comparing their preferred  $\text{Lin}(Z_L)/\text{Lin}(Z_A)^2$  to their alternative  $Z_L/\text{Lin}(Z_A)^2$  is essentially the same as comparing  $\text{Lin}(Z_L)/\text{Lin}(Z_A)^2$  (partially linearized) to  $Z_L/Z_A^2$  (not linearized).



To allow a direct comparison with others, our not-linearized results have changed somewhat from those reported in the conference proceedings [14] and the original preprint of this article which calculated the not-linearized result for  $Z_R$  and  $Z_N$  as  $(\alpha_s^c(m_b^*)/\alpha_s^c(q^*))^{p_{0,L}^c} Z_X^{cl}$  rather than  $C_L^{fc} Z_X^{cl}$ .

In Table VI we show the coefficients of the individual  $B_B$  parameters for the three different linearizations described, both with and without tadpole improvement. Table VII shows the corresponding value for  $\hat{B}_B$  at both one-loop and at two-loops. The variation among the three different linearizations of the non-tadpole-improved coefficients is much larger than for the tadpole-improved coefficients. Because there are equal numbers of quarks in the numerator and denominator, the individual  $B_B$  parameters should be independent of the wave-function normalization of both the heavy and the light quarks. This implies that the coefficients should be independent of tadpole improvement. Tables VI and VII show that this is only true for the fully-linearized quantity,  $\text{Lin}(Z_L/Z_A^2)$ .

From Table VI, the overall change in  $B_B(m_b^*)$  for the three different linearizations, when calculated with the tadpole-improved coefficients, is 20%. However, when calculated from non-tadpole-improved perturbative coefficients,  $B_B(m_b^*)$  can change by a much larger factor. This suggests that the order- $\alpha^2$  effects may be large. While these can be treated in a variety of ways, we think that they can be treated well or treated poorly. For example, the use of tadpole improvement stabilizes the central values and reduces statistical errors. The UKQCD collaboration did not use tadpole improvement, which suggests that their perturbative coefficients may be unnecessarily sensitive to their choice of linearization. (Their preferred choice is what we call “partially linearized”; they also considered what we call “not linearized”.) Their decision not to use tadpole-improvement was forced upon them by the way they implemented the light-quark field rotations which were required to remove  $O(a)$  corrections to matrix elements [15].

We rank the various organizations of perturbation theory in decreasing order of preference: fully linearized, not linearized, partially linearized. We discuss, in turn, several (related) disadvantages with partial linearizing: larger relative statistical errors, increased sensitivity to the value of the lattice coupling constant (via choice of prescription), and non-optimal handling of order- $\alpha^2$  terms. Firstly, due to the larger off-diagonal coefficients in the terms of the sum in Eq. (4.13b), the numerical result for  $B_B(m_b^*)$  using non-tadpole-improved partially-linearized coefficients (the last row of Table VI) has a larger relative statistical error than do the results from the other choices of linearization.

Secondly, we studied the stability of the results from three groups: the  $\beta = 6.2$  clover-static UKQCD simulation [21], the  $\beta = 6.0$  clover-static Giménez & Martinelli simulation [45], and our  $\beta = 6.0$  Wilson-static simulation (both tadpole-improved and not-tadpole improved). All three of these groups that have done static  $B_B$  simulations used slightly different ways of evaluating the perturbative coefficients. We have analyzed all simulation data consistently to facilitate comparisons of the results. We compared the linearizations for two lattice couplings ( $\tilde{\alpha}$  and  $\alpha_V(q^*a = 2.18)$ ) and for summing the logarithms (à la renormalization-group (RG) techniques) *versus* not summing the logarithms. These are discussed further in Sec. VI. We see the same trends in each group’s data. Each group’s partially-linearized result is less stable under variations of  $\alpha$  than is their not linearized or fully linearized. Their fully-linearized result is close to their not-linearized result; these are 20% higher than their partial-linearized result.

Method	$Z_{BL}$	$Z_{BR}$	$Z_{BN}$	$Z_{BS}$	$B_B(m_b^*)$
With Tadpole Improvement					
$\text{Lin}(Z_X/Z_A^2)$	$1.070^{+0.009}_{-0.009}$	$-0.022^{+0.001}_{-0.001}$	$-0.202^{+0.008}_{-0.012}$	$-0.137^{+0.006}_{-0.008}$	$0.98^{+0.04}_{-0.04}$
$(Z_X/Z_A^2)$	$1.066^{+0.020}_{-0.016}$	$-0.031^{+0.002}_{-0.004}$	$-0.275^{+0.021}_{-0.037}$	$-0.246^{+0.013}_{-0.025}$	$0.96^{+0.04}_{-0.04}$
$\text{Lin}(Z_X)/\text{Lin}(Z_A)^2$	$1.003^{+0.014}_{-0.021}$	$-0.041^{+0.003}_{-0.005}$	$-0.371^{+0.026}_{-0.050}$	$-0.251^{+0.015}_{-0.021}$	$0.80^{+0.04}_{-0.04}$
Without Tadpole Improvement					
$\text{Lin}(Z_X/Z_A^2)$	$1.070^{+0.009}_{-0.008}$	$-0.022^{+0.001}_{-0.001}$	$-0.202^{+0.008}_{-0.012}$	$-0.137^{+0.006}_{-0.007}$	$0.98^{+0.04}_{-0.04}$
$(Z_X/Z_A^2)$	$1.030^{+0.011}_{-0.014}$	$-0.043^{+0.004}_{-0.007}$	$-0.384^{+0.036}_{-0.065}$	$-0.343^{+0.018}_{-0.042}$	$0.87^{+0.04}_{-0.04}$
$\text{Lin}(Z_X)/\text{Lin}(Z_A)^2$	$0.802^{+0.039}_{-0.082}$	$-0.059^{+0.005}_{-0.010}$	$-0.529^{+0.049}_{-0.092}$	$-0.358^{+0.025}_{-0.044}$	$0.49^{+0.04}_{-0.04}$

TABLE VI. The effects of different linearizations on the coefficients: The errors on the coefficients are the statistical errors of varying the parameters  $q^*a$ ,  $a^{-1}$ ,  $m_b^*$ , and  $\Lambda_{\text{QCD}}^{(5)}$  by 20% from our preferred values. The error bars on  $B_B(m_b^*)$  are the bootstrap errors.  $B_B(m_b^*)$  is the chiral extrapolation of the “combine-then-fit” values from Eq. (2.7).

Method	$B(4.33)$	$n_f$	one-loop		two-loop	
			$\Lambda$	$\hat{B}_B$	$\Lambda$	$\hat{B}_B$
With Tadpole Improvement						
$\text{Lin}(Z_X/Z_A^2)$	0.98(4)	5	175	1.40(6)	175	1.50(6)
		4	226	1.36(6)	246	1.46(6)
$(Z_X/Z_A^2)$	0.96(4)	5	175	1.37(6)	175	1.47(6)
		4	226	1.33(6)	246	1.43(6)
$\text{Lin}(Z_X)/\text{Lin}(Z_A)^2$	0.80(4)	5	175	1.14(6)	175	1.23(6)
		4	226	1.11(6)	246	1.19(6)
Without Tadpole Improvement						
$\text{Lin}(Z_X/Z_A^2)$	0.98(4)	5	175	1.40(6)	175	1.50(6)
		4	226	1.36(6)	246	1.46(6)
$(Z_X/Z_A^2)$	0.87(4)	5	175	1.24(6)	175	1.34(6)
		4	226	1.21(6)	246	1.30(6)
$\text{Lin}(Z_X)/\text{Lin}(Z_A)^2$	0.49(4)	5	175	0.70(6)	175	0.75(6)
		4	226	0.68(6)	246	0.73(6)

TABLE VII. From the  $B_B(m_b^*)$  result extracted by Monte Carlo, listed in Table VI, we calculated a  $\hat{B}_B$  with both 4 and 5 flavors (see text). The  $\text{Lin}(Z_X/Z_A^2)$  results are our preferred values. As mentioned in the text,  $\hat{B}_B$  varies with  $n_f$  and  $\Lambda^{(n_f)}$  as well as with loop-order.

Thirdly, we believe that partial linearization does a poor job of organizing higher-order terms. The treatment of  $O(\alpha^2)$  terms in partially-linearized coefficients causes the low values seen by all groups by linearizing some terms but not the whole ratio. We prefer the fully-linearized method because it removes all of these  $O(\alpha^2)$  terms (as in a Taylor expansion) by linearizing the whole ratio. Fully- or not-linearizing the coefficients treats the  $O(\alpha^2)$  terms more appropriately than does partially linearizing.

Our preferred choice of linearization (full) can also be motivated by the non-perturbative renormalization method, introduced by the Rome-Southampton group [46]. The non-perturbative renormalization method for  $B_B$  parameter would be very similar to that used to obtain the renormalization constants for the kaon  $B$  parameter [47,48], in which all the factors of the lattice wave function normalization of the quarks cancel explicitly for the  $B$  parameter. In perturbation theory, this corresponds to our preferred full linearization. The non-perturbative method only determines the lattice part of the renormalization factor; a choice of linearization would still have to be made for the continuum factor. However, the continuum factor can and should be calculated to next to leading order [46], making it less sensitive to the different choices of linearizations.

In summary, our preference for the treatment of the coefficients is to fully linearize the ratio (in the notation of this section,  $Z_{B_L}$  is  $\text{Lin}(Z_L/Z_A^2)$ ). This gives a result which has no order- $\alpha^2$  terms, which is insensitive to the inclusion of tadpole improvement and to the wave-function normalization model by allowing explicit cancelations, and which reduces the statistical errors in  $B_B$ . The quantitative consequences of our choice are discussed in the following section where we compare the results of different groups.

Just as the numerical value of  $B_B$  is stable because of cancelations of correlated fluctuations in numerator and denominator, we have argued that so too are its perturbative corrections when fully linearized. The fully-linearized perturbatively-calculated coefficients for  $B_B$  are likely more reliable than those for the product  $B_B f_B^2$ , the quantity which is required in the analysis of  $\overline{B^0}-B^0$  mixing experiments. In the Appendix, we discuss our recommendation for how to linearize the product  $B_B f_B^2$ .

## VI. WORLD COMPARISON

In Table VIII (IX), we show a collection of results from several groups scaled to give  $B_B(m_b^*)$ ,  $B_B(2.0 \text{ GeV})$ , and the one-loop (two-loop) renormalization-group-invariant  $\hat{B}_B$  parameter. Results from both static and relativistic-quark simulations are shown. The simulations using relativistic heavy Wilson quarks [2,3,49,50] calculate the  $B_B$  parameter for quark masses around charm and extrapolate up to the physical mass, using a fit model of the form

$$B_B = B_B^0 + \frac{B_B^1}{M} \quad (6.1)$$

The value of  $B_B^0$  should be the same as the static theory result. (It is better to do a combined analysis of relativistic and static quarks to obtain a value for  $B_B$ .) We call  $B_B^0$  the “extrapolated-static” value.

Tables VIII and IX show that values for  $B_B$  obtained from Wilson action simulations are basically consistent; the small differences can be explained by small lattice-spacing and

Method	Ref.	$\beta$	$\mu_2$ (GeV)	$B(\mu_2)$	$n_f$	$\Lambda$ (MeV)	$B(2.0)$	one-loop $B(4.33)$	$\hat{B}_B$
Static-Clover	[21]	6.2	$m_b=5.0$	$0.69(4)$	5	130	-	-	$1.02(6)$
					4	200	$0.75(4)$	$0.70(4)$	$0.98(6)$
Static-Clover	[21]	6.2	$m_b=5.0$	$0.81(4)$	5	130	-	-	$1.19(6)$
					4	200	$0.87(4)$	$0.82(4)$	$1.14(6)$
Static-Clover	[45]	6.0	$m_b=5.0$	$0.54(4)$	5	151	-	-	$0.79(6)$
					4	200	$0.59(4)$	$0.55(4)$	$0.77(6)$
Static-Clover	[45]	6.0	$m_b=5.0$	$0.76(5)$	5	151	-	-	$1.11(7)$
					4	200	$0.82(5)$	$0.77(5)$	$1.08(7)$
Static-Wilson	this work	6.0	$m_b^*=4.33$	$0.98(4)$	5	175	-	$0.98(4)$	$1.40(6)$
					4	226	$1.05(4)$		$1.36(6)$
Extrap. Static	[2]	5.7-6.3	$\mu=2.0$	$1.04(5)$	4	200	$1.04(5)$	$0.97(5)$	$1.36(7)$
					4	226		$0.97(5)$	$1.34(6)$
Extrap. Static	[49]	6.4	$\mu=3.7$	$0.90(5)$	0	200	$0.94(5)$	$0.89(5)$	$1.21(7)$
					4	200	$0.95(5)$	$0.89(5)$	$1.25(7)$
Wilson-Wilson	[2]	5.7-6.3	$\mu=2.0$	$0.96(6)$	4	200	$0.96(6)$	$0.90(6)$	$1.25(8)$
					4	226		$0.89(6)$	$1.24(8)$
Wilson-Wilson	[2,3]	6.1	$\mu=2.0$	$1.01(15)$	4	200	$1.01(15)$	$0.94(13)$	$1.32(20)$
					4	226		$0.94(14)$	$1.30(19)$
Wilson-Wilson	[50]	6.1	$m_b=5.0$	$0.895(47)$	0	239	$0.96(5)$	$0.90(5)$	$1.21(6)$
					4	239	$0.98(5)$	$0.91(5)$	$1.25(7)$
					5	183	-	-	$1.29(7)$
Wilson-Wilson	[50]	6.3	$m_b=5.0$	$0.840(60)$	0	246	$0.90(6)$	$0.85(6)$	$1.14(8)$
					4	246	$0.92(6)$	$0.85(6)$	$1.17(8)$
					5	189	-	-	$1.20(9)$
Wilson-Wilson	[49]	6.4	$\mu=3.7$	$0.86(5)$	0	200	$0.90(5)$	$0.85(5)$	$1.16(7)$
					4	200	$0.91(5)$	$0.85(5)$	$1.19(7)$
Sum Rule	[51]		$m_b=4.6$	$1.00(15)$	5	175	-	-	$1.43(22)$
					4	227	$1.08(16)$	$1.00(15)$	$1.39(21)$

TABLE VIII. The authors' numbers, quoted at the listed value for  $\mu_2$ , have been scaled using Eq. (4.19) to  $\mu=2.0$  GeV and to  $m_b^*=4.33$  GeV. The *slanted* numbers are those that the cited authors quote. We calculated  $B_B(m_b^*)$  in the Static-Wilson case and then scaled it to 2.0 GeV using  $n_f=4$  and calculated a  $\hat{B}_B$  with both 4 and 5 flavors (see text). The value quoted by this work uses the fully-linearized tadpole-improved coefficients. The JLQCD collaboration cite their  $\Lambda$ 's as  $n_f=0$  values. When Abada *et al.* quotes a  $\hat{B}_B$  for the Wilson quarks, they use  $n_f=0$ . We scaled both groups' results using both  $n_f=0$  and  $n_f=4$ .

Method	Ref.	$\beta$	$\mu_2$ (GeV)	$B(\mu_2)$	$n_f$	$\Lambda$ (MeV)	two-loop		
							$B(2.0)$	$B(4.33)$	$\hat{B}_B$
Static-Clover	[21]	6.2	$m_b=5.0$	$0.69(4)$	5	130	-	-	1.09(6)
					4	200	0.74(5)	0.70(4)	1.05(6)
Static-Clover	[21]	6.2	$m_b=5.0$	$0.81(4)$	5	130	-	-	1.27(6)
					4	200	0.86(4)	0.81(4)	1.23(6)
Static-Clover	[45]	6.0	$m_b=5.0$	$0.54(4)$	5	136	-	-	0.86(6)
					4	200	0.58(4)	0.54(4)	0.82(6)
Static-Clover	[45]	6.0	$m_b=5.0$	$0.76(5)$	5	136	-	-	1.21(8)
					4	200	0.77(5)	0.81(5)	1.16(8)
Static-Wilson	this work	6.0	$m_b^*=4.33$	$0.98(4)$	5	175	-	0.98(4)	1.50(6)
					4	246	1.04(4)		1.46(6)
Extrap. Static	[2]	5.7-6.3	$\mu=2.0$	$1.04(5)$	4	200		0.98(5)	1.49(7)
					4	246	1.04(5)	0.98(5)	1.46(7)
Extrap. Static	[49]	6.4	$\mu=3.7$	$0.90(5)$	0	200	0.93(5)	0.89(5)	1.29(7)
					4	200	0.94(5)	0.89(5)	1.35(7)
Wilson-Wilson	[2]	5.7-6.3	$\mu=2.0$	$0.96(6)$	4	200		0.91(6)	1.37(9)
					4	246	0.96(6)	0.90(6)	1.35(9)
Wilson-Wilson	[2,3]	6.1	$\mu=2.0$	$1.01(15)$	4	200		0.96(14)	1.44(21)
					4	246	1.01(15)	0.95(14)	1.42(21)
Wilson-Wilson	[50]	6.1	$m_b=5.0$	$0.895(47)$	0	239	0.94(5)	0.90(5)	1.29(7)
					4	239	0.96(5)	0.90(5)	1.35(7)
					5	183	-	-	1.36(7)
Wilson-Wilson	[50]	6.3	$m_b=5.0$	$0.840(60)$	0	246	0.88(6)	0.85(6)	1.21(9)
					4	246	0.90(6)	0.85(6)	1.26(9)
					5	189	-	-	1.30(9)
Wilson-Wilson	[49]	6.4	$\mu=3.7$	$0.86(5)$	0	200	0.89(5)	0.85(5)	1.24(7)
					4	200	0.90(5)	0.85(5)	1.29(7)
Sum Rule	[51]		$m_b=4.6$	$1.00(15)$	5	175	-	-	1.54(23)
					4	227	1.07(16)	1.00(15)	1.50(22)

TABLE IX. This table repeats the analysis in Table VIII, using the *two-loop* renormalization group invariant  $B_B$  parameter.

$B_B(4.33 \text{ GeV})$	UKQCD [21]	G&M [45]	TAD	NO-TAD
fl (M3)	$\Sigma \tilde{\alpha}$	0.84(5)	0.85(4)	0.97(4)
	$\frac{\alpha_V}{\tilde{\alpha}}$	0.83(5)	0.85(3)	0.97(4)
	$\Sigma \tilde{\alpha}$	0.75(5)	0.84(4)	0.96(4)
	$\frac{\alpha_V}{\tilde{\alpha}}$	0.77(5)	0.84(3)	0.96(4)
nl (M1)	$\Sigma \tilde{\alpha}$	0.85(5)	0.84(3)	0.95(4)
	$\frac{\alpha_V}{\tilde{\alpha}}$	0.82(5)	0.82(3)	0.96(4)
	$\Sigma \tilde{\alpha}$	0.78(5)	0.83(3)	0.94(4)
	$\frac{\alpha_V}{\tilde{\alpha}}$	0.76(5)	0.81(3)	0.95(4)
pl (M2)	$\Sigma \tilde{\alpha}$	0.72(5)	0.70(3)	0.75(4)
	$\frac{\alpha_V}{\tilde{\alpha}}$	0.62(4)	0.62(3)	0.80(4)
	$\Sigma \tilde{\alpha}$	0.60(4)	0.68(3)	0.73(4)
	$\frac{\alpha_V}{\tilde{\alpha}}$	0.54(4)	0.61(3)	0.78(4)

TABLE X. Comparison between the fit-then-combine (Eq. (2.6)) analysis for  $B(m_b)$  of the three groups’ data. These numbers are for  $m_b = 4.33 \text{ GeV}$ ,  $q^* = 2.18a^{-1}$ , and  $n_f = 5$ . “fl” is fully-linearized, “nl” is not-linearized, and “pl” is partially-linearized. “M1,” “M2,” and “M3” refer to the notation of Giménez & Martinelli [45] and Wittig [52]. We list both our tadpole-improved (TAD) and our non-tadpole-improved (NO-TAD) results. The errors are roughly estimated from statistical errors on the raw  $B_X$  values and approximate errors on the coefficients. See the text for comments on  $\tilde{\alpha}$  and  $\alpha_V$ .

finite-volume effects. Our result is consistent with that of Bernard and Soni, as reported by Soni [2], for the extrapolated static Wilson fermions.

Since the original appearance of the preprint for this article (hep-lat/9610026, version 1), data has been made available which allows a more detailed comparison between ourselves (on the high end of the world results) and others (on the low end). Firstly, we have added the updated numbers from Giménez & Martinelli [45] to Tables VIII and IX. Secondly, we note that Wittig [52] has a nice review on the subject of leptonic decays of lattice heavy quarks, in which he compares the results of UKQCD [21], Giménez & Martinelli [45] and the preprint of this article.

In his Sec. 4.2, Wittig offers Table 9 for comparison, using our non-tadpole-improved results. We find that the tadpole-improved Wilson results improve the non-tadpole-improved results, so we prefer to compare their clover-improved results to our tadpole-improved results. Our analogous comparison results in the numbers listed in Table X.

In the comparison, we use  $n_f = 5$  and  $\Lambda_{\text{QCD}}^{(5)} = 0.175 \text{ GeV}$  which result in  $\alpha_s^{\text{cont}}(m_b = 4.33 \text{ GeV}) = 0.21$ . We also use our two-loop  $\Lambda_V a = 0.169$  to scale  $\alpha_V^{\text{latt}}(q^* = 2.18a^{-1}) = 0.18$ . Both  $\alpha_s$  are with two-loops from Eq. (4.15). We also compare using  $\tilde{\alpha} = 6/(4\pi\beta u_0^4)$ , which is 0.132 for the UKQCD collaboration [21], 0.1458 for Giménez & Martinelli [45], and 0.198 for us. (For each group, we used  $u_0 = 1/8\kappa_{\text{crit}}$  to calculate  $\tilde{\alpha}$ .) In addition, since the

original UKQCD results<sup>3</sup> do not sum the logarithms (à la RG techniques), Table X lists both summing logs ( $\Sigma$ ) and not summing the logs ( $\mathbb{Z}$ ).

Rather than calculate a  $q^*a$  (Eq. (4.17)) and a  $\Lambda_V a$  (Eq. (4.14)) for the clover action, we used our values. Since  $\alpha_V$  is a function of  $(q^*a/\Lambda_V a)$ ,  $\alpha_V(q^*)$  is the same for all three groups. We note that  $a^{-1} = 2.9$  was used for UKQCD and  $a^{-1} = 2.1$  was used for both Giménez & Martinelli and ourselves. Since  $q^*a$  was chosen to be 2.18 for all three groups, the scales in the comparison of Table X are different. This is the reason that the UKQCD  $\mathbb{Z}$  results differ from their  $\Sigma$  results. The  $\mathbb{Z}$  results are more sensitive to the scale of the perturbative matching.

Though not listed in the table, we are able to reproduce the results of both UKQCD [21] and Giménez & Martinelli [45] for  $m_b = 5.0$  GeV,  $\mu = a^{-1}$ ,  $n_f = 4$ , and  $\Lambda_{\text{QCD}}^{(4)} = 0.200$  GeV when we tailor the respective calculations according to the method presented in each paper<sup>4</sup>. Also, we agree with the results of Wittig [52] for our  $\Sigma$ - $\alpha_V$  entries when we use his parameters.

Both UKQCD's and Giménez's & Martinelli's quoted values for the static  $B_B$  are lower than all of the other results. One possible reason for these low results is that they used the clover action for the light quarks, which does not have corrections to the continuum limit that are linear in the lattice spacing, whereas the standard Wilson fermion action does have such artifact terms. However, the Wilson results are stable over four different lattice spacings, which implies that the lattice artifact terms alone cannot account for the difference between the clover results and the Wilson numbers.

Table X shows that the not-linearized (and fully-linearized) static clover results for  $B_B$  are larger than the partially-linearized results, as is discussed in the original papers. The clover-static results that use the not-linearized matching are in better agreement, though still low, with the results from simulations which use relativistic heavy quarks to simulate the  $b$  quark (see Table VIII). All the published data [2,49] on calculating  $B_B$  using relativistic heavy quarks favor a negative value of  $B_B^1$  in Eq. (6.1). For consistency, the static value of  $B_B$  should be higher than the value of  $B_B$  extrapolated to the  $b$  quark mass. This is true for our result and favors the higher clover-static results.

The various choices made in the calculation have non-negligible effects. One can choose which action to use (Wilson vs clover), whether or not to tadpole-improve, and which linearization method to use. The choice between our tadpole-improved Wilson-static action and the non-tadpole-improved clover-static action has a 15% effect in both the fully- and not-linearized ( $\Sigma$ - $\alpha_V$ ) cases. This is a 20% effect for the partially-linearized case. In addition, tadpole-improvement stabilizes the Wilson-static results to the extent that one can make a

---

<sup>3</sup>UKQCD did investigate the use of renormalization group improved perturbation theory, but they did not use it to calculate their final results.

<sup>4</sup>To reproduce UKQCD's [21] 0.69(4) and 0.81 (the latter is our conversion of their quoted  $\hat{B} = 1.19$ ), do not sum the logs, use  $\mu a = 1$ , and do not include the cross term,  $(U^T)_{LS}^c$ , in the coefficient of  $\mathcal{O}_L$ . To reproduce Giménez' & Martinelli's [45] Table 3, sum the logs and include the cross term, but use  $\mu a = 1$ , even for the  $\alpha_V(q^*a = 2.18)$  case.

better comparison of different linearizations between tadpole-Wilson-static and clover-static than between non-tadpole-Wilson-static and clover-static. Finally, there is a 20% effect due to choice of linearization for either action. This linearization effect is at least as large as the effect due to choice of action. For reasons given in Sec. V, our favorite choice of linearization is the fully-linearized treatment.

A similar trend can be seen in each group's results: partially-linearized values are smaller and less stable than either not-linearized or fully-linearized values. This is due to  $O(\alpha^2)$  terms which may or may not cancel to varying degrees. The partially-linearized treatment only linearizes part of the ratio which causes its value to be misleadingly low. The not-linearized and fully-linearized treatments are better because they do not do this. The fully-linearized treatment is preferred because it treats  $O(\alpha^2)$  terms uniformly by removing them (as one does in an expansion).

## VII. CONCLUSION

Our primary result from this tadpole-improved  $\beta = 6.0$  Wilson-static calculation is  $B_B(m_b^*) = 0.98_{-4-18}^{+4+3}$ , where the errors are statistical (bootstrap) and systematic, respectively. The overall systematic error is obtained in quadrature from the following:  $_{-3}^{+3}$  from the choice of fit-range,  $_{-2}^{+1}$  from the parameter-dependence of the perturbative-calculated mixing coefficients, and  $_{-18}^{+0}$  due to the choice of linearization of the coefficients, as was discussed in Sec. V. The unusual asymmetry of the latter systematic error reflects our preference for a particular choice of linearization ("full"). Our second favorite choice ("not-linearized") results in a central value of 0.96. We quote a very conservative systematic error to encompass our least favorite choice (0.80 from "partial linearization") even though we have argued against this choice. Systematic errors from finite lattice spacing and from quenching are not estimated.

Tables VIII and IX show that values for  $B_B$  obtained from Wilson action simulations are basically consistent; the small differences can be explained by small lattice-spacing and finite-volume effects. The simulations all favor a negative value of  $B_B^1$  in Eq. (6.1) [2]. For consistency, this implies that the static value of  $B_B$  should be higher than the value of  $B_B$  extrapolated to the  $b$  quark mass. Our number is on the high end of the comparison in Table VIII and is consistent with that of Bernard and Soni [2] who use extrapolated static Wilson fermions.

In Sec. V we investigated the effect of changing the way the four-fermion operator renormalization and the axial-current renormalization were combined to form the matching coefficient for the  $B_B$  parameter. We presented arguments that suggested that our preferred way of organizing the continuum-to-lattice matching (full linearization) was superior to any other method we considered. We also showed that making a different choice could lower the result by as much as 20%. Besides the linearizations, Table X shows a 15% difference due to choice of action between our tadpole-improved  $\beta = 6.0$  Wilson-static and the non-tadpole-improved  $\beta = 6.0$  and 6.2 clover-static results in the fully- and not-linearized cases. (The Wilson results are at the high end of the world data and the clover results are at the low end.) Partial-linearization leaves a 20% effect due to choice of action. The effect due to choice of linearization is at least as large as the effect due to choice of action.



Although all organizations of perturbation theory at one-loop are theoretically equal, some are more equal than others! Fully linearizing gives a result which has no order- $\alpha^2$  terms and which is insensitive to the inclusion of tadpole improvement and to the wave-function normalization model by allowing explicit cancelations (which reduces the statistical errors in  $B_B$ ).

In our perturbative-matching procedure we included next-to-leading order log terms and organized the perturbative matching in a way that we believe reduces higher-order corrections. Also we used the automatic scale-setting procedure of Lepage and Mackenzie to find the “best” scale to use in the lattice-to-continuum matching. The agreement of our results with relativistic heavy quark results supports our procedure. Our conclusion is that for the Wilson-static case, the use of tadpole improvement and of a fully-linearized treatment of the mixing coefficients is preferred. Of course, this may become less important numerically with increased coupling and/or improved actions; however, we still recommend the procedure.

Although sensible things can be done to reduce the effects of higher-order perturbative corrections in the lattice-to-continuum matching, this will remain the dominant uncertainty in the calculation of  $B_B$  in the static theory. In principle, “all” that is required is a calculation of the two-loop anomalous dimension of the  $\mathcal{O}_L$  and  $A_\mu$  operators on the lattice. Although this calculation is very difficult, new developments in lattice perturbation theory for Wilson quarks [53] and a new stochastic way of doing lattice perturbation theory [54] may make these calculations more tractable in the future. A more immediate solution would be to use the numerical renormalization technique, developed by the Rome-Southampton group [46], which has already been used to determine the lattice perturbative coefficients for static  $f_B$  [48], for the kaon  $B_K$  parameter [47], and for other important quantities.

The relative consistency of the Wilson  $B_B$  results motivates a large study using both relativistic and static quarks in the same simulations to constrain the interpolation to the  $B$  mass. To constrain the systematic errors, the results of simulations with different lattice spacings and volumes should be combined to take the continuum limit. This kind of study will also help to control the perturbative-matching errors, as the effects of the higher-order perturbative terms are reduced as the continuum limit is taken. (A nice example of this for the effects of different renormalization prescriptions on light-quark decay constants has been given by the GF11 group [55].)

Once mixing in the  $\overline{B}_s^0$ – $B_s^0$  system has been measured experimentally, the results can be combined with data from  $\overline{B}^0$ – $B^0$  mixing experiments to calculate the  $V_{ts}/V_{td}$  ratio of CKM matrix elements. The advantage of calculating this ratio is that various uncertain standard-model factors cancel. However, a value of  $B_{B_s}f_{B_s}^2/B_Bf_B^2$  is required. As there are a large number of lattice results on the calculation of  $f_{B_s}/f_B$  [10], here we concentrate on the ratio  $B_{B_s}/B_B$ .

Using a fit model which is linear in the quark mass, we obtain  $B_{B_s}/B_B = 0.99^{+1}_{-1}(1)$ . (The first error is statistical (bootstrap) and the second is the standard deviation of the fitted value for “reasonable choices” of fit range.) Even though the ratio  $B_{B_s}/B_B$  is determined quite precisely, it is not resolved whether  $B_{B_s}$  is greater than or less than  $B_B$  since the  $B_B$  parameter is found to depend weakly on the quark mass. Other groups [21,50,56] have reported similar findings. Most lattice simulations have found that  $f_{B_s}$  is between ten and twenty percent larger than  $f_B$  [10]. Bernard *et al.* [56] have extracted the ratio of

$B_s f_{B_s}^2 / B_B f_B^2$  directly by doing individual fits to the three-point function in relativistic quark simulations. This is a promising approach for relativistic heavy quarks. We did not try it because of concerns about the signal-to-noise ratio and about the size of the perturbative coefficients in the static theory.

Our result also contains an unknown systematic error due to quenching. Quenched chiral perturbation theory predicts the effects of quenching to be small for  $B_B$  [57,58]; this conclusion was confirmed by Bernard and Soni [2] who calculated  $B_B$  in both quenched and dynamical simulations. In Soni's review [2] of the lattice calculation of weak matrix elements at the *Lattice '95* conference, he quotes a value of  $B_B(2 \text{ GeV}) = 1.0 \pm 0.15$  (90% confidence) as his best estimate of the  $B_B$  parameter. Our result,  $B_B(2 \text{ GeV}) = 1.05^{+4+3}_{-4-19}$ , is consistent with this value and with the vacuum-saturation-approximation value, 1.

## ACKNOWLEDGMENTS

This work is supported in part by the U.S. Department of Energy under grant numbers DE-FG05-84ER40154 and DE-FC02-91ER75661, and by the University of Kentucky Center for Computational Sciences. The computations were carried out at NERSC.

## APPENDIX: LINEARIZATION STRATEGY FOR $B_B f_B^2$

In the analysis of  $\overline{B}^0 - B^0$  mixing experiments the value of  $B_B f_B^2$  is required. Here we discuss the linearization options for combining  $B_B$  and  $f_B$  from a variety of linearizations of these quantities. If a not-linearized  $B_B$  is multiplied with a not-linearized  $(f_B)^2$ , then the only order- $\alpha^2$  effects which remain are due specifically to not linearizing the numerator of  $B_B$ . We estimate this effect to be on the order of 10%. If one multiplies a partially-linearized  $B_B$  with a linearized  $f_B$ ,  $\text{Lin}(Z_A)^2$ , then there should be no order- $\alpha^2$  effects due to the product. However, if one mixes a linearized with a not-linearized  $B_B$  and  $f_B$ , then there can be terms of almost 20%. Although the difference between  $Z_A$  and  $\text{Lin}(Z_A)$  is smaller than 5%, the difference between  $\text{Lin}(Z_A)^2$  and  $\text{Lin}(Z_A^2)$  is just over 15%. The practical drawback of using a  $B_B$  which is not linearized or is partially linearized is that there are order- $\alpha^2$  terms present which may or may not cancel when the  $B_B$  is combined with an  $f_B$ .

The practical drawback to using the fully-linearized  $B_B$  is linearizing the product  $B_B f_B^2$ . This is easily remedied. The fully-linearized  $B_B$ ,  $B_{fl}$ , essentially has the form

$$B_{fl} = (1 + \alpha^c A + \alpha^l C) B^{raw} \quad (\text{A1})$$

where the  $B_R$ ,  $B_N$ , and  $B_S$  can be included by adjusting the values of  $A$  and  $C$  appropriately. When this is combined with the square of the linearized  $f$ ,

$$f_{lin} = (1 + \alpha^c D + \alpha^l E) f^{raw} \quad (\text{A2})$$

it would be convenient to get a linearized result with no order- $\alpha^2$  terms:

$$(1 + \alpha^c A + \alpha^l C + 2\alpha^c D + 2\alpha^l E) B^{raw} (f^{raw})^2 \quad (\text{A3})$$

Since

$$(1 + \alpha A) \left( 1 + \alpha \frac{B}{1 + \alpha A} \right) = (1 + \alpha A + \alpha B) \quad (\text{A4})$$

this is straightforward to accomplish. The product of  $B_{fl}$  with the linearized square of

$$f'_{lin} = \left( 1 + \alpha^c \frac{D}{\left( \frac{B_{fl}}{B_L^{raw}} \right)} + \alpha^l \frac{E}{\left( \frac{B_{fl}}{B_L^{raw}} \right)} \right) f^{raw} \quad (\text{A5})$$

gives Eq. (A3) with no order- $\alpha^2$  terms due to coefficient multiplication. Our  $B_L^{raw}$  value can be read from the first row of Table I.

While the product of the partially-linearized  $B_B$  with the linearized  $f_B$  also does not have any order- $\alpha^2$  terms due to coefficient multiplication, the partially-linearized  $B_B$  by itself has order- $\alpha^2$  terms which are on the order of 18% (See Tables VI and VII). The advantage of our method is that all three quantities  $B_B(m_b^*)$ ,  $f_B(m_b^*)$  and  $B_B f_B^2(m_b^*)$  have no order- $\alpha^2$  terms due to coefficient multiplication, and that  $B_B(m_b^*)$  is stable against the inclusion of tadpole improvement and the choice of wave-function normalization.

## REFERENCES

- [1] J. Rosner, J. Phys. G: Nucl. Part. Phys. **18**, 1575 (1992), for example.
- [2] A. Soni, in *Lattice '95*, Proceedings of the International Symposium, Melbourne, Australia, 1995, edited by T. Kieu *et al.* (*Nucl. Phys. B (Proc. Suppl.)* ) **47**, 43, (1996) and references therein.
- [3] C. Bernard, T. Draper, G. Hockney, and A. Soni, Phys. Rev. D **38**, 3540 (1988).
- [4] J. Flynn, in *Lattice '96*, Proceedings of the International Symposium, St Louis, USA, 1996, edited by C. Bernard *et al.* (*Nucl. Phys. B (Proc. Suppl.)* ) **53**, 168, (1997).
- [5] C. R. Allton *et al.*, Nucl. Phys. **B349**, 598 (1991).
- [6] E. Eichten, G. Hockney, and H. B. Thacker, in *Lattice '89*, Proceedings of the International Symposium, Capri, Italy, 1989, edited by N. Cabibbo *et al.* (*Nucl. Phys. B (Proc. Suppl.)* ) **17**, 529, (1990).
- [7] J. M. Flynn, O. F. Hernández, and B. R. Hill, Phys. Rev. D **43**, 3709 (1991).
- [8] G. P. Lepage, in *Lattice '91*, Proceedings of the International Symposium, Tsukuba, Japan, 1991, edited by M. Fukugita *et al.* (*Nucl. Phys. B (Proc. Suppl.)* ) **26**, 45, (1992).
- [9] C. Bernard, in *Lattice '93*, Proceedings of the International Symposium, Dallas, Texas, 1993, edited by T. Draper *et al.* (*Nucl. Phys. B (Proc. Suppl.)* ) **34**, 47, (1994).
- [10] C. Allton, in *Lattice '95*, Proceedings of the International Symposium, Melbourne, Australia, 1995, edited by T. Kieu *et al.* (*Nucl. Phys. B (Proc. Suppl.)* ) **47**, 31, (1996).
- [11] A. Duncan *et al.*, Phys. Rev. D **51**, 5101 (1994).
- [12] T. Draper and C. McNeile, in *Lattice '93*, Proceedings of the International Symposium, Dallas, Texas, 1993, edited by T. Draper *et al.* (*Nucl. Phys. B (Proc. Suppl.)* ) **34**, 453, (1994).
- [13] T. Draper and C. McNeile, in *Lattice '95*, Proceedings of the International Symposium, Melbourne, Australia, 1995, edited by T. Kieu *et al.* (*Nucl. Phys. B (Proc. Suppl.)* ) **47**, 429, (1996).
- [14] J. Christensen, T. Draper, and C. McNeile, in *Lattice '96*, Proceedings of the International Symposium, St Louis, USA, 1996, edited by C. Bernard *et al.* (*Nucl. Phys. B (Proc. Suppl.)* ) **53**, 378, (1997).
- [15] (UKQCD Collaboration) C. R. Allton *et al.*, Nucl. Phys. **B407**, 331 (1993).
- [16] A. Duncan, E. Eichten, G. Hockney, and H. Thacker, in *Lattice '91*, Proceedings of the International Symposium, Tsukuba, Japan, 1991, edited by M. Fukugita *et al.* (*Nucl. Phys. B (Proc. Suppl.)* ) **26**, 391, (1992).
- [17] C. Bernard, C. M. Heard, J. Labrenz, and A. Soni, in *Lattice '91*, Proceedings of the International Symposium, Tsukuba, Japan, 1991, edited by M. Fukugita *et al.* (*Nucl. Phys. B (Proc. Suppl.)* ) **26**, 384, (1992).
- [18] T. Bhattacharya, R. Gupta, G. Kilcup, and S. Sharpe, Phys. Rev. D **53**, 6486 (1995).
- [19] C. A. Dominguez and N. Paver, Phys. Lett. B **293**, 197 (1992).
- [20] (Particle Data Group) R. M. Barnett *et al.*, Phys. Rev. D **54**, S1 (1996).
- [21] (UKQCD Collaboration) A. K. Ewing *et al.*, Phys. Rev. D **54**, 3526 (1996).
- [22] A. J. Buras and P. H. Weisz, Nucl. Phys. **B333**, 66 (1990).
- [23] G. P. Lepage and P. B. Mackenzie, Phys. Rev. D **48**, 2250 (1993).
- [24] M. Ciuchini *et al.*, Z. Phys. **C68**, 239 (1995).
- [25] M. Ciuchini, E. Franco, and V. Giménez, Phys. Lett. **388B**, 167 (1996).

- [26] G. Buchalla, Phys. Lett. **395B**, 364 (1997).
- [27] A. J. Buras, M. Jamin, M. E. Lautenbacher, and P. H. Weisz, Nucl. Phys. **B370**, 69 (1992).
- [28] M. Neubert, Phys. Rep. **245**, 259 (1994).
- [29] G. Buchalla, A. J. Buras, and M. E. Lautenbacher, Rev. Mod. Phys. **68**, 1125 (1996).
- [30] V. Giménez, Nucl. Phys. **B401**, 116 (1993).
- [31] X. Ji and M. J. Musolf, Phys. Lett. **257B**, 409 (1991).
- [32] D. J. Broadhurst and A. G. Grozin, Phys. Lett. **267B**, 105 (1991).
- [33] D. J. Broadhurst and A. G. Grozin, Phys. Lett. **274B**, 421 (1992).
- [34] V. Giménez, Nucl. Phys. **B375**, 582 (1992).
- [35] A. J. Buras, M. Jamin, and P. H. Weisz, Nucl. Phys. **B347**, 491 (1990).
- [36] E. Eichten and B. Hill, Phys. Lett. **240B**, 193 (1990).
- [37] O. F. Hernández and B. R. Hill, Phys. Rev. D **50**, 495 (1994).
- [38] E. Eichten and B. Hill, Phys. Lett. **234B**, 511 (1990).
- [39] A. Borrelli and C. Pittori, Nucl. Phys. **B385**, 502 (1992).
- [40] C. Morningstar, Phys. Rev. D **50**, 5902 (1994).
- [41] J. Sloan, in *Lattice '94*, Proceedings of the International Symposium, Bielefeld, Germany, 1994, edited by F. Karsch *et al.* (Nucl. Phys. B (Proc. Suppl.) **42**, 171, 1995).
- [42] C. Sachrajda, in *Lattice '95*, Proceedings of the International Symposium, Melbourne, Australia, 1995, edited by T. Kieu *et al.* (Nucl. Phys. B (Proc. Suppl.) **47**, 100, 1996).
- [43] G. S. Bali and K. Schilling, Phys. Rev. D **47**, 661 (1993).
- [44] C. T. H. Davies *et al.*, Phys. Rev. D **50**, 6963 (1994).
- [45] V. Giménez and G. Martinelli, Phys. Lett. **398B**, 135 (1997).
- [46] G. Martinelli *et al.*, Nucl. Phys. **445**, 81 (1995).
- [47] A. Donini *et al.*, Phys. Lett. **360B**, 83 (1995).
- [48] A. Donini *et al.*, in *Lattice '95*, Proceedings of the International Symposium, Melbourne, Australia, 1995, edited by T. Kieu *et al.* (Nucl. Phys. B (Proc. Suppl.) **47**, 489, 1996).
- [49] A. Abada *et al.*, Nucl. Phys. **B376**, 172 (1992).
- [50] JLQCD collaboration, in *Lattice '95*, Proceedings of the International Symposium, Melbourne, Australia, 1995, edited by T. Kieu *et al.* (Nucl. Phys. B (Proc. Suppl.) **47**, 433, 1996).
- [51] S. Narison and A. A. Pivovarov, Phys. Lett. **327B**, 341 (1994).
- [52] H. Wittig, Leptonic decays of heavy quarks on the lattice, hep-lat/9705034, 1997.
- [53] G. Burgio, S. Caracciolo, and A. Pelissetto, Nucl. Phys. **B478**, 687 (1996).
- [54] F. D. Renzo *et al.*, Nucl. Phys. **B426**, 675 (1994).
- [55] F. Butler *et al.*, Nucl. Phys. **B421**, 217 (1994).
- [56] C. Bernard, T. Blum, and A. Soni, in *Lattice '96*, Proceedings of the International Symposium, St Louis, USA, 1996, edited by C. Bernard *et al.* (Nucl. Phys. B (Proc. Suppl.) **53**, 382, 1997).
- [57] M. J. Booth, Phys. Rev. D **51**, 2338 (1995).
- [58] S. Sharpe and Y. Zhang, Phys. Rev. D **53**, 5125 (1995).

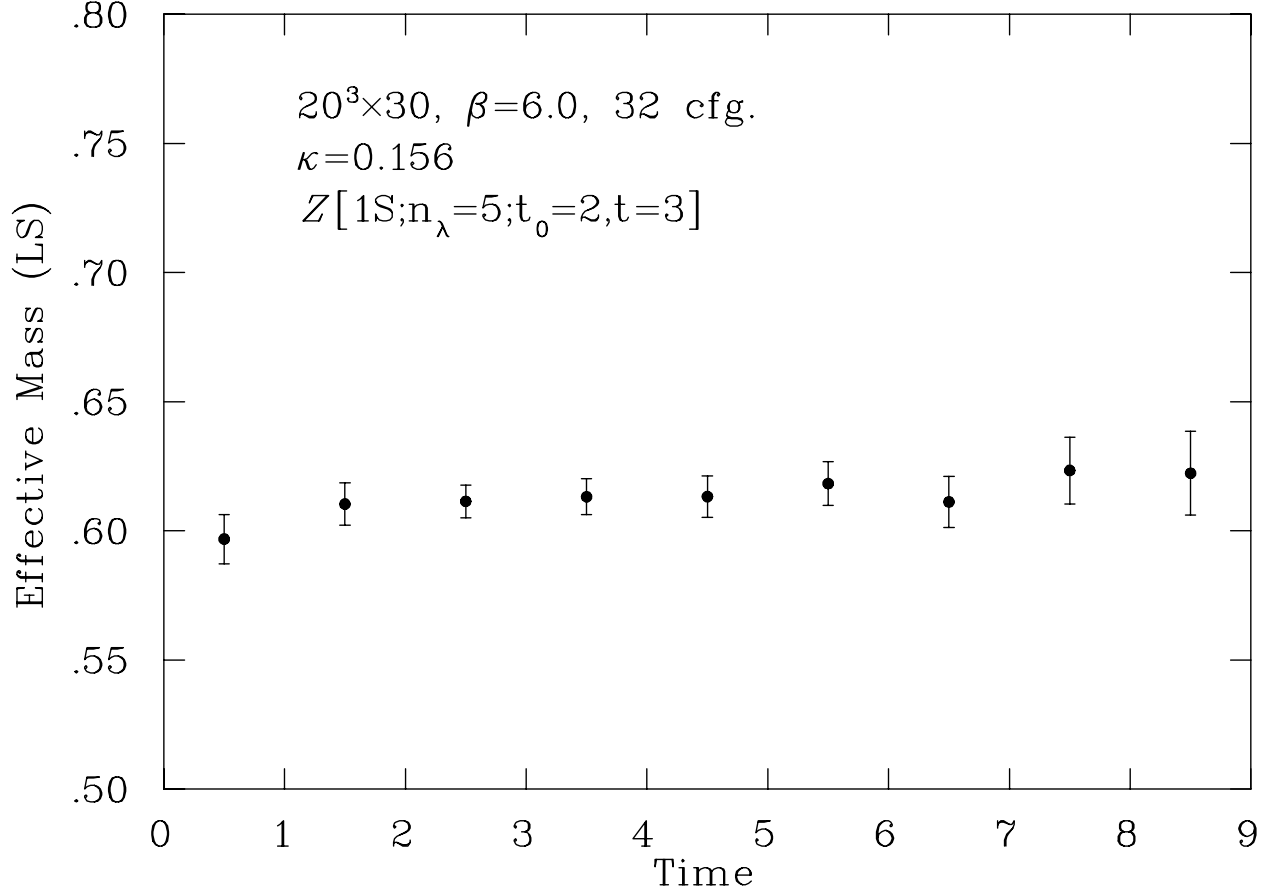


FIG. 1. Effective mass  $m(t + 1/2) = \ln C(t)/C(t + 1)$  from the LS (local sink, smeared source) two-point correlation function  $C(t)$ . The source was smeared with an optimal smearing function produced by the MOST [12] algorithm which was designed to eliminate excited-state contamination.

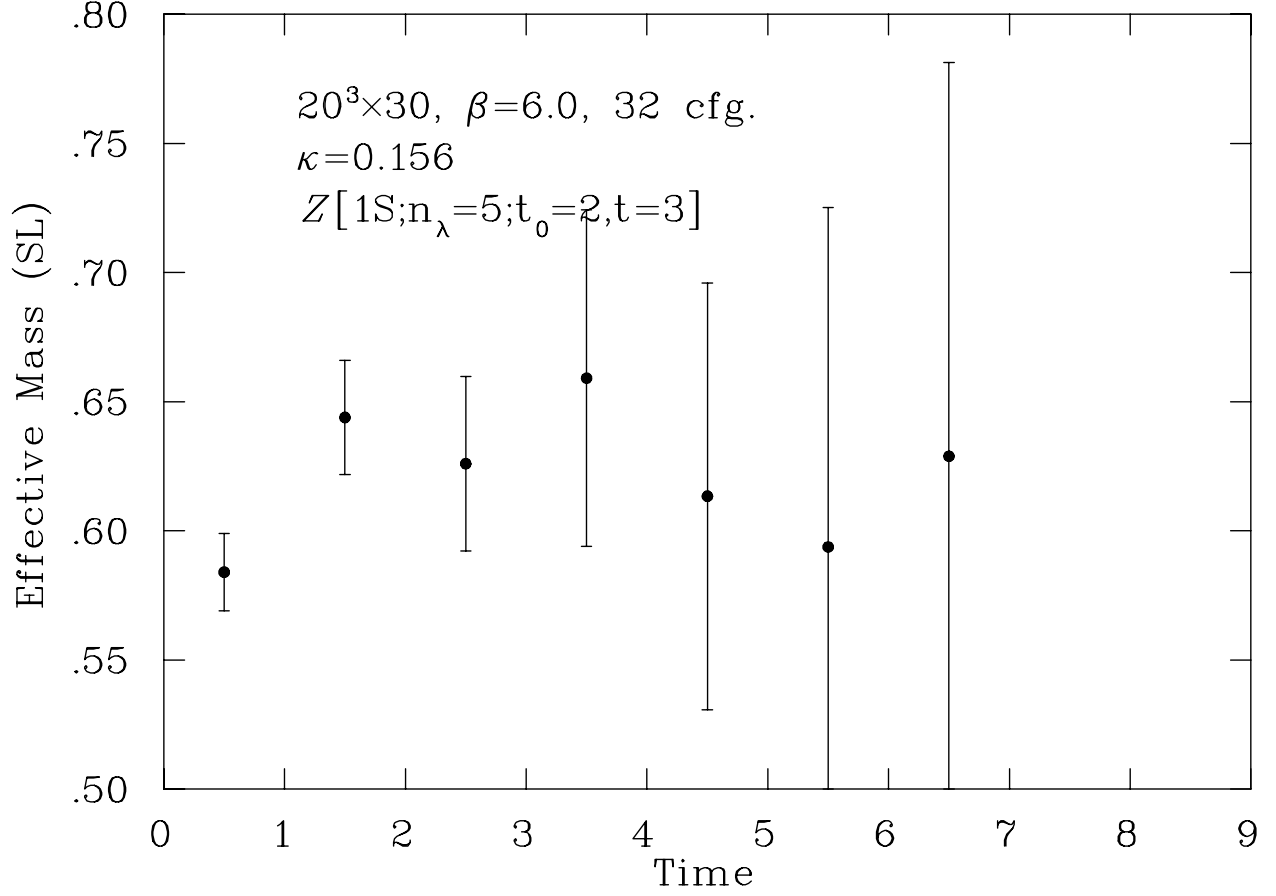


FIG. 2. Same as for Fig. 1 but for the SL (smeared sink, local source) two-point correlation function. The same optimal smearing function is used to eliminate excited state contamination, but statistical errors are larger since the source is (necessarily) a delta function.

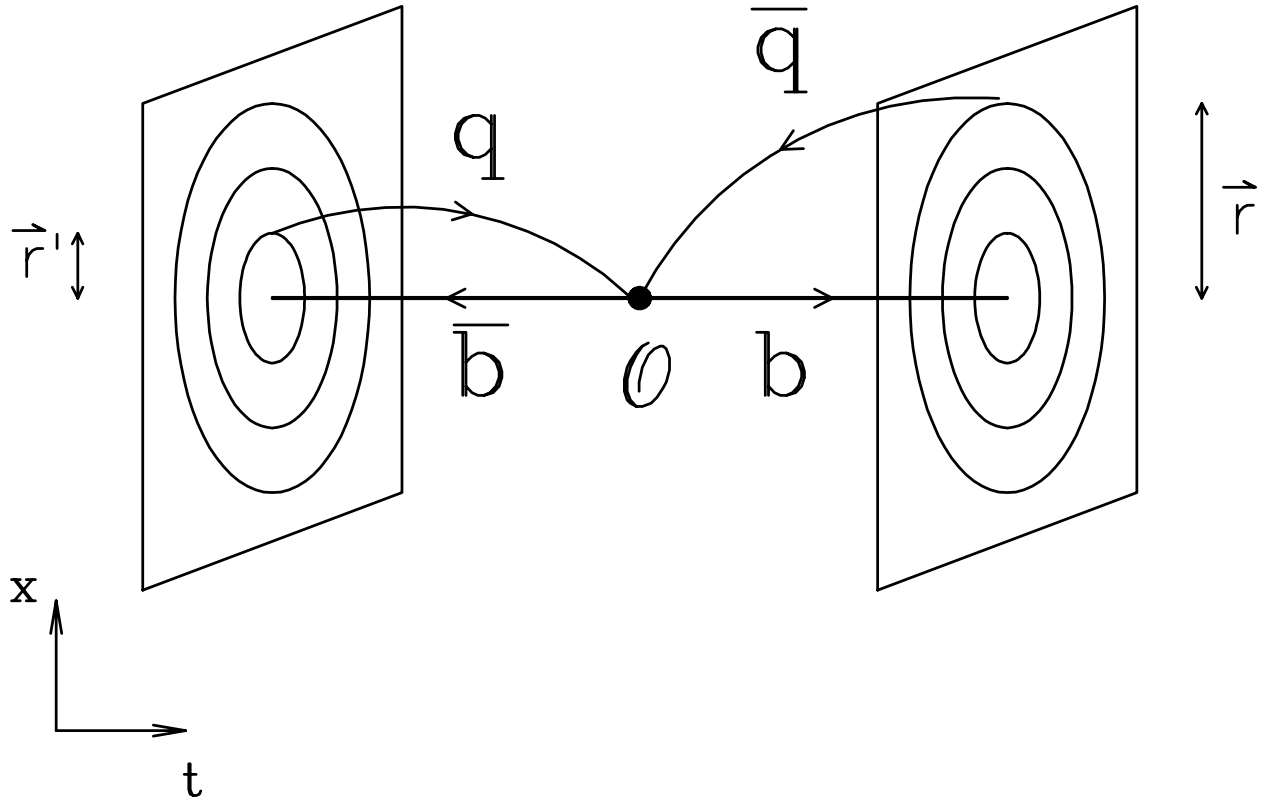


FIG. 3. Schematic diagram of the quark flow for the three-point correlation function of Eq. (2.1). The “targets” are intended to represent the smearing of the light quark relative to the static quark. The static quarks are restricted to the spatial origin.



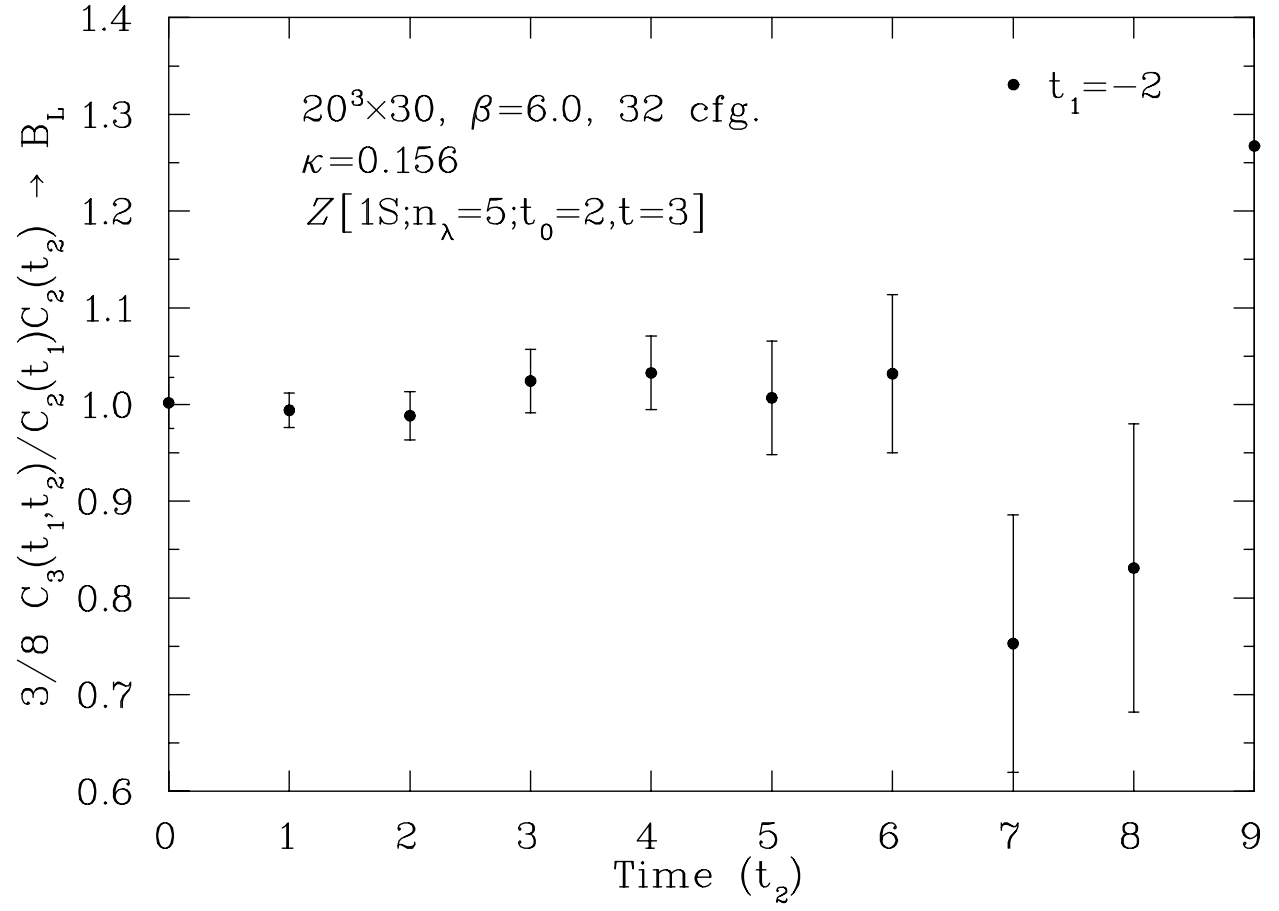


FIG. 4. Raw  $B$  parameter for the  $\mathcal{O}_L$  operator from Eq. (2.5).

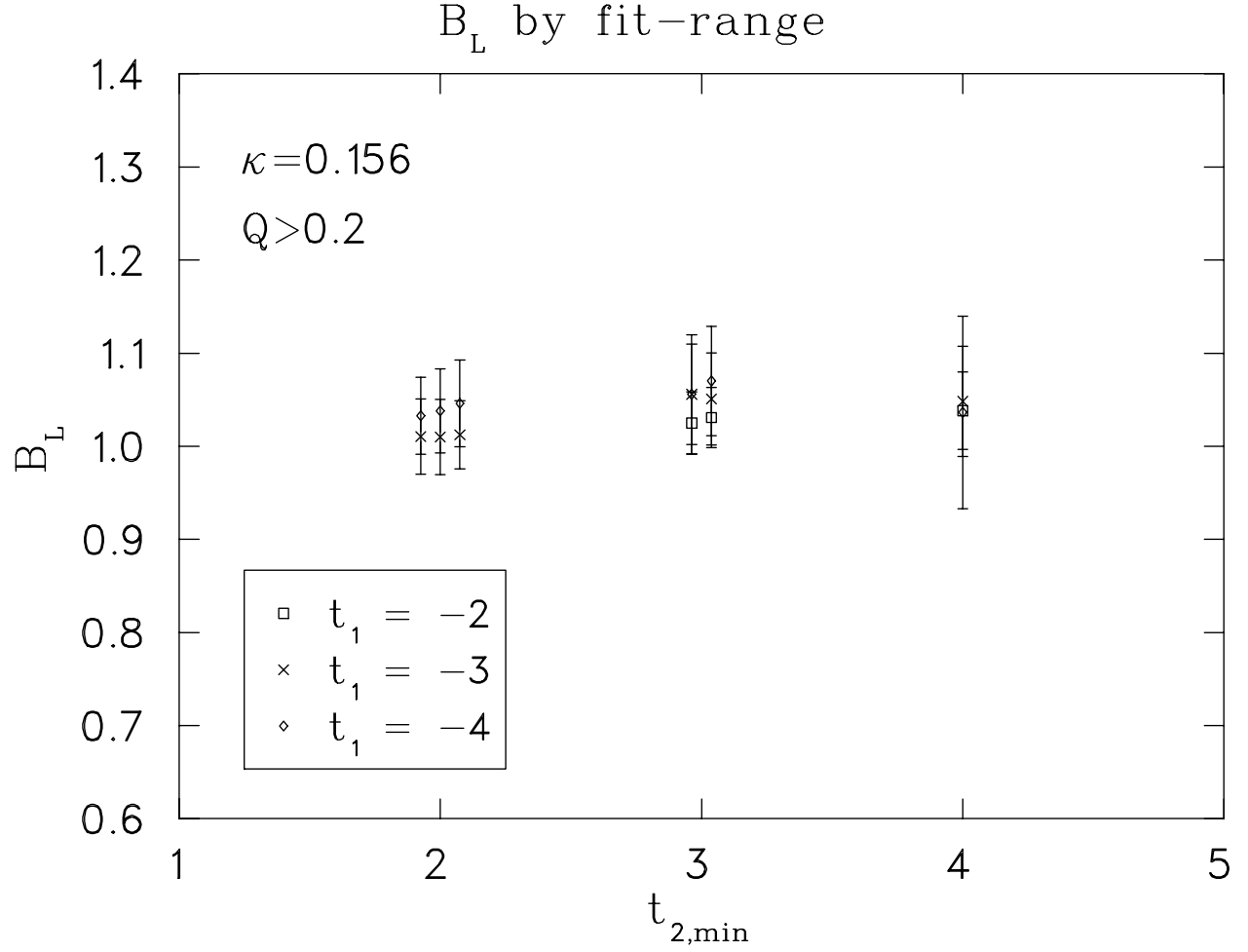


FIG. 5. The dependence on the fitted raw  $B_L$  parameter on the choice of  $t_1$ , the (fixed) time position of one interpolating field, and on the fit range  $t_{2,\min} - t_{2,\max}$  of the other. Clustered points have different  $t_{2,\max}$ . All fits take into account correlations in  $t_2$ , and are not displayed if the naive quality of fit  $Q$  does not exceed 0.2.

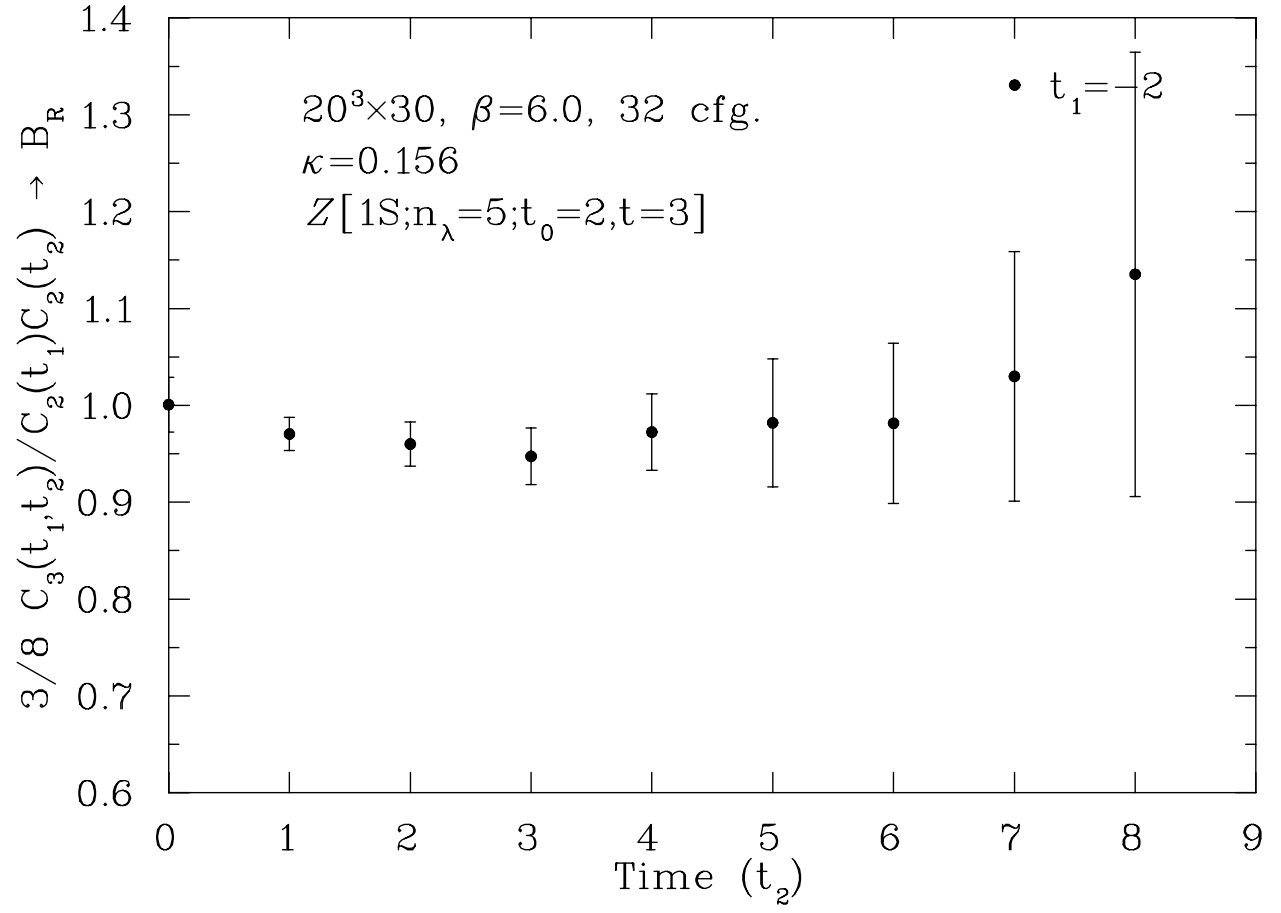


FIG. 6. Same as for Fig. 4 but for the  $\mathcal{O}_R$  operator.

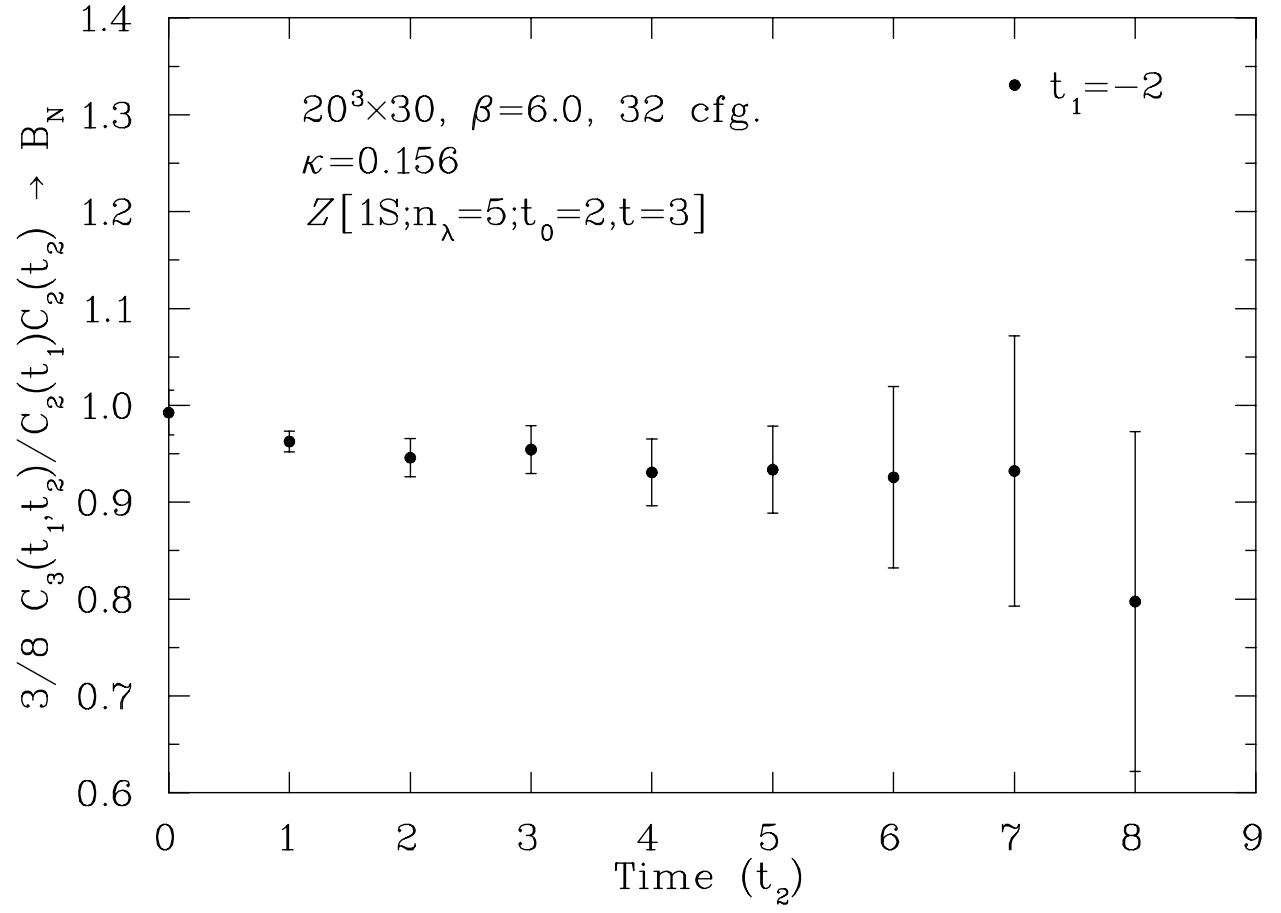


FIG. 7. Same as for Fig. 4 but for the  $\mathcal{O}_N$  operator.

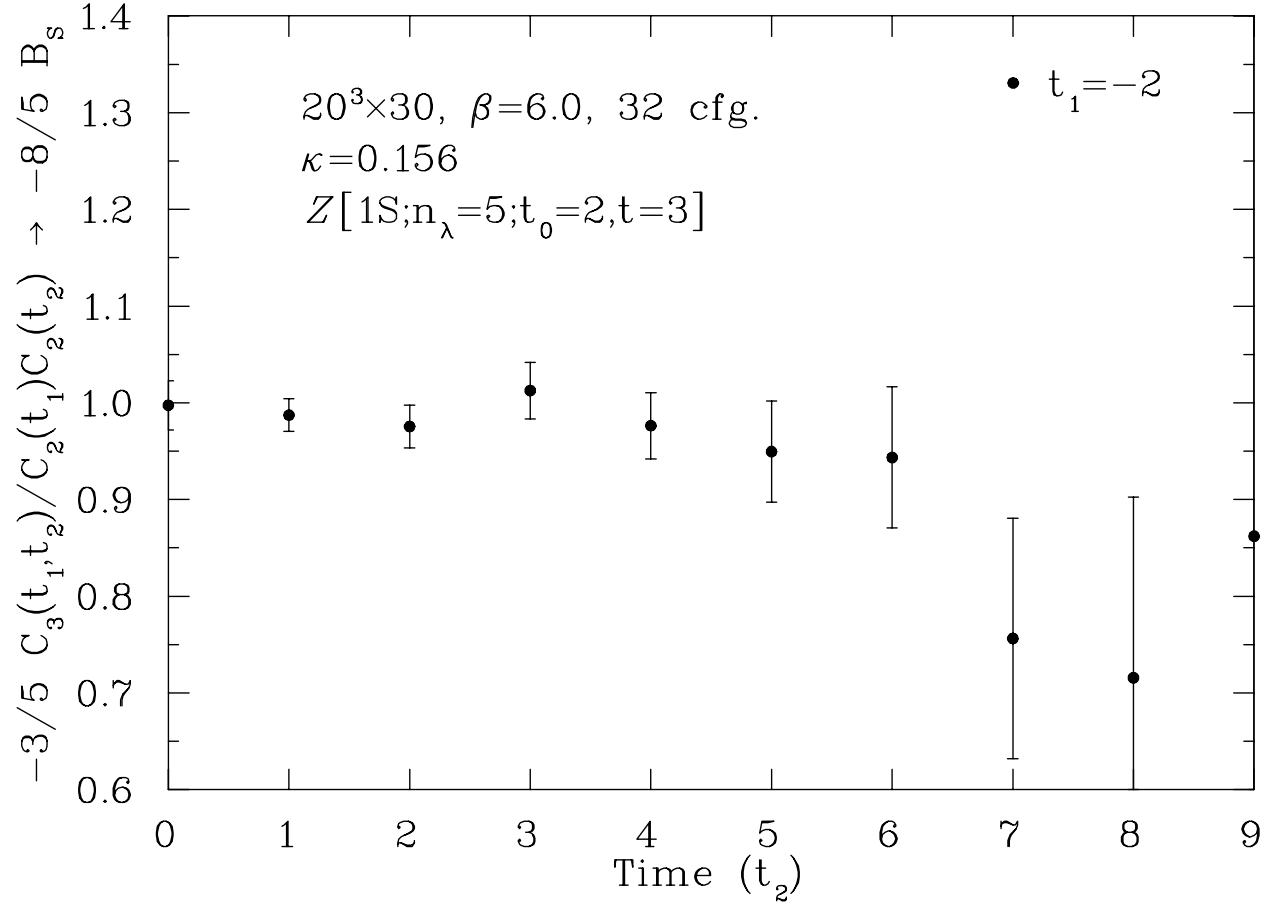


FIG. 8. Same as for Fig. 4 but for the  $\mathcal{O}_S$  operator. Note the normalization as explained in Table I.

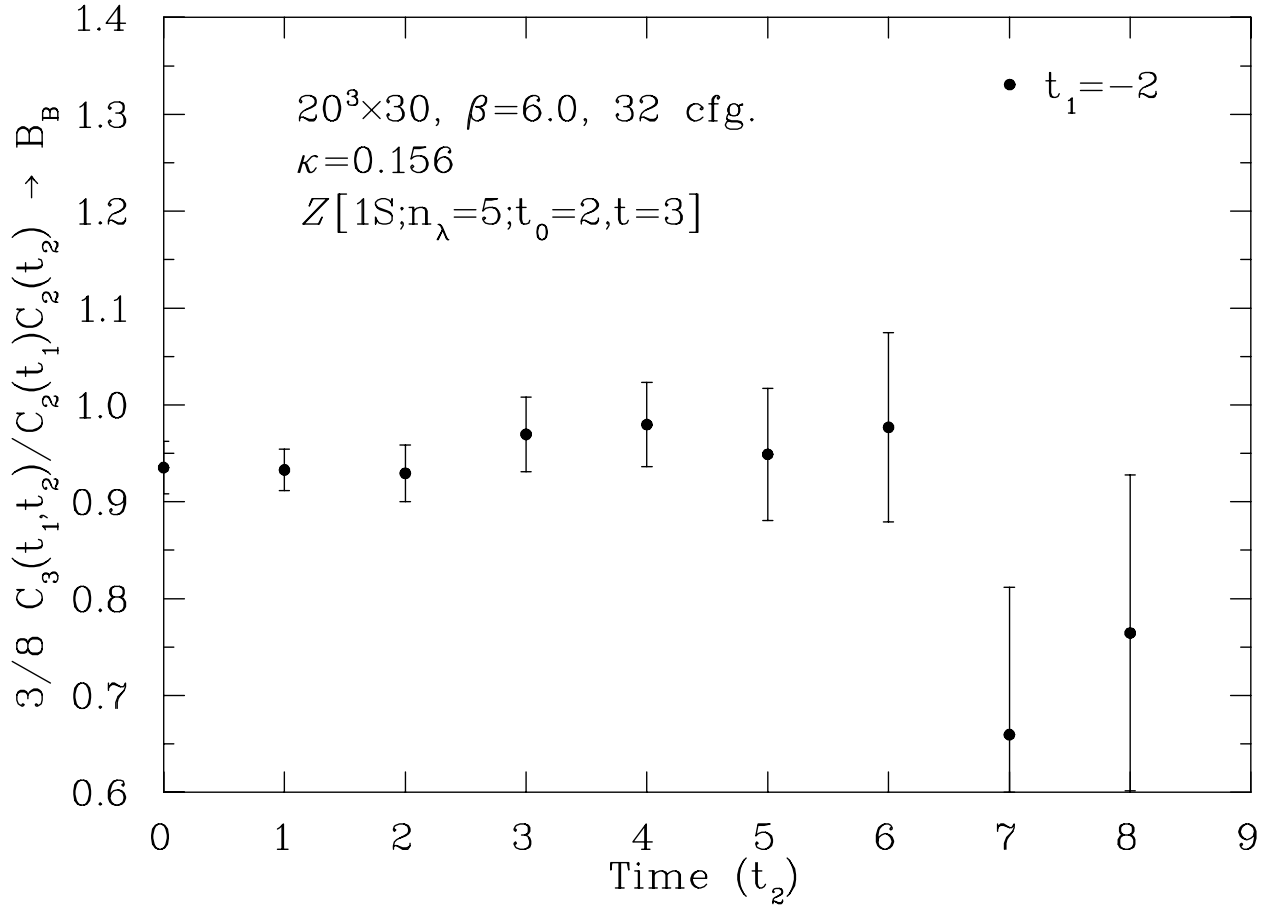


FIG. 9. The ratio of (the linear combination of) three-point functions to two-point functions which approaches  $B_B$  for large Euclidean times.

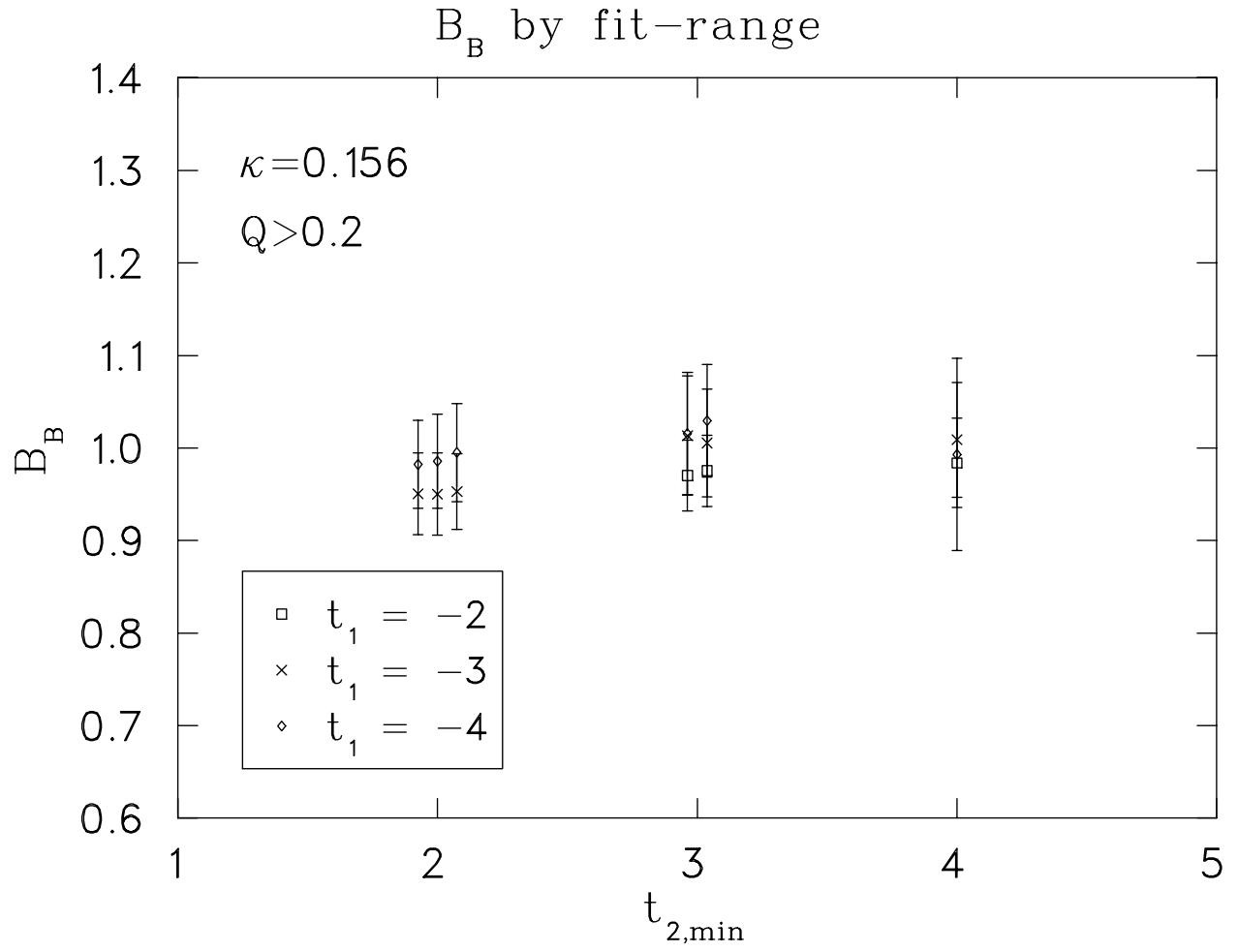


FIG. 10. Same as for Fig. 5 but for the  $B_B$  parameter itself.